Cambridge Environmental Research Consultants

In Association With:

CERC activities under the TOPFARM project: Wind turbine wake modelling using ADMS

Final report

Prepared for

Risø DTU, National Laboratory for Sustainable Energy

13th January 2011

CERC

Report Information

CERC Job Number:	FM766
Job Title:	CERC activities during the TOPFARM project: Wind turbine wake modelling using ADMS
Prepared for:	Risø DTU, National Laboratory for Sustainable Energy
Report Status:	Final
Report Reference:	FM766/2011/1
Issue Date:	13th January 2011

Author(s):	Amy Stidworthy, David Carruthers, Julian Hunt

Reviewer(s):	David Carruthers

Issue	Date	Comments
1	13/01/11	

Main File(s):	FM766_TOPFARM_R1_13Jan2011_Final.docx
Figures and Tables	Model Run Reference(s)

Contents

Summary

During the TOPFARM project CERC have developed a new fast and efficient approach to the problem of modelling the development of wind turbine wakes. The similarities between the dispersion of a plume of gaseous material in the atmospheric boundary layer and the breakdown of a wind turbine wake have been exploited.

New developments have been made to CERC's ADMS model that is used worldwide for modelling the dispersion of atmospheric pollutants for regulatory purposes. In these new developments, the fully-expanded turbine wake is characterised as a thin volume source, with source strength and dimensions calculated to give a maximum wind speed deficit $2aU$. Here a is the Axial Induction Factor calculated either from an iterative solution of Blade Element Momentum (BEM) theory, or, from the input values of thrust coefficient as a function of the hub height wind speed U, according to the user's choice. Meandering-induced turbulence is modelled using ADMS's well-validated model of concentration fluctuations, here used as a surrogate for velocity fluctuations. The changes to ADMS include consideration of the special dispersion characteristics of wind turbine wakes: the downstream delay before the wake vortex begins to entrain ambient air, the additional shear-induced turbulence at the edge of the wake and the lack of large-scale wind direction meandering in wind farm environments.

Wind farms can be modelled easily in the new model, with the individual sources being modelled in downstream order, so that wakes from upstream turbines affect the vertical wind and turbulence profiles used both to characterise the turbine effective sources and to disperse their wakes. Special treatment is included for the wakes of turbines that are inside the wakes of upstream turbines: increased turbulence and no entrainment delay. Output from the model is in the form of hourly values of ambient wind and power, wake-affected wind and power, wind and power deficits and meandering-induced turbulence on a user-defined grid of output points and/or at the turbine locations. These data can be given either individually for each meteorological condition modelled, or, as an average wind speed and total power over the full set of meteorological data modelled. The new model has been validated against measured data from Tjæreborg Enge, Nysted wind farm and Noordzee wind farm.

1. Introduction

This report describes the activities of CERC under the EU FP6-funded project TOPFARM.

Work at CERC has centred on the application of CERC's widely used ADMS model to the problem of modelling the wake behind a wind turbine and the interaction of wakes in a wind farm environment. ADMS is used worldwide for modelling the dispersion of pollutants released into the atmosphere; the standard model is described briefly in Section 2.

There are many similarities between the behaviour of a wind turbine wake and the behaviour of a plume, which have been exploited here. The change in concentration of a pollutant due to a release of that pollutant is used as a surrogate for the change in the wind speed due to a wind turbine. The fluctuations in concentration due to short length scale 'meandering' of the plume are used as a surrogate for velocity fluctuations due to wake meandering. The ADMS fluctuations model is well-established and well-validated and includes the interaction between plumes (or wakes). The application of ADMS to wind turbine wake modelling, the modifications made to account for areas where plumes and wakes behave differently and the extension of the application to whole wind farms are described in Section 3. The advantage of using a model such as ADMS for this type of problem is that it is very quick to run on a standard desktop PC, making it ideal for the type of wind farm design optimisation tool envisaged in TOPFARM.

Another work package in TOPFARM was responsible for collecting and analysing available measurements from wind turbines and wind farms. These have been used here to validate the application of ADMS to wind turbine wake modelling. Two datasets of wake measurements behind a single turbine from Tjæreborg Enge in Denmark have been simulated. One of these included LIDAR measurements of turbulence in the wake, which have been compared with the velocity fluctuations output from ADMS. Two datasets of power deficits at turbines inside a wind farm have been simulated: Nysted wind farm and NoordZee wind farm. This validation work is described in detail in Section 4.

Finally, Section 5 contains some conclusions and an outline of future work.

2. The ADMS model

ADMS is a practical, short-range dispersion model that simulates a wide range of types of releases to the atmosphere either individually or in combination. It is a “new generation” dispersion model using two parameters, namely the boundary layer height *h* and the Monin-Obukhov length L_{MO}, to describe the atmospheric boundary layer and using a skewed Gaussian concentration distribution to calculate dispersion under convective conditions. The model is applicable up to 60 km downwind of the source and provides useful information for distances up to 100 km.

ADMS has been extensively validated and full technical specification documents are publicly available; for these the reader is referred to the References section at the end of this document.

Users of ADMS include private companies, public bodies, government departments and universities all over the world. ADMS is recognised as the world-leading software for industrial pollution modelling.

ADMS is supplied with a comprehensive User Interface, integrated links to Graphical Information System (GIS) software and contour plotting packages, and a detailed User Guide. CERC run scheduled and customised training courses for model users. Users with a support contract may make use of the CERC helpdesk; the team of expert users are able to offer personalised help and advice to users.

ADMS is developed and maintained solely by CERC, where the latest research in the field is applied to increase the number of model features, improve model results, improve the user’s experience and reduce model run times.

3. Application of ADMS to the modelling of wind turbine wakes

Similarities between the decay of the wake behind a wind turbine in operation and the dispersion of a plume of passive gas emitted from an elevated source have been exploited in the application of ADMS to the modelling of wind turbine wakes.

A plume is characterised by an amount of gas emitted continuously, which is advected downwind whilst mixing with the ambient air, at a rate determined by the amount of turbulence in the atmosphere. A wind turbine wake is characterised by a wind speed deficit downwind of the turbine, which is also advected downwind and gradually mixes with the ambient air, in a similar manner to a plume, but with some special characteristics.

The ADMS model of concentration fluctuations is used here as a surrogate for velocity fluctuations, giving as output the component of along-wind turbulent velocity induced by the meandering wake.

Section 3.1 describes how ADMS has been applied to the problem of modelling the wake downwind of a single turbine; section 3.2 describes how this has been extended to whole wind farms.

3.1 Single turbine

3.1.1 Characterisation of the effective source

Classical 1-D momentum theory for a wind turbine (see Hansen, Chapter 4) states that the rate of change of momentum across a turbine rotor disc (i.e. the thrust) is caused solely by the pressure gradients across the disc, and that since the pressure recovers at some distance downstream, the momentum in the 'stream-tube' upstream of this pressure gradient is the equal to the momentum in the stream-tube downstream of the pressure gradient, i.e. the stream-tube expands as the flow speed reduces. This is demonstrated schematically in Figure 1.

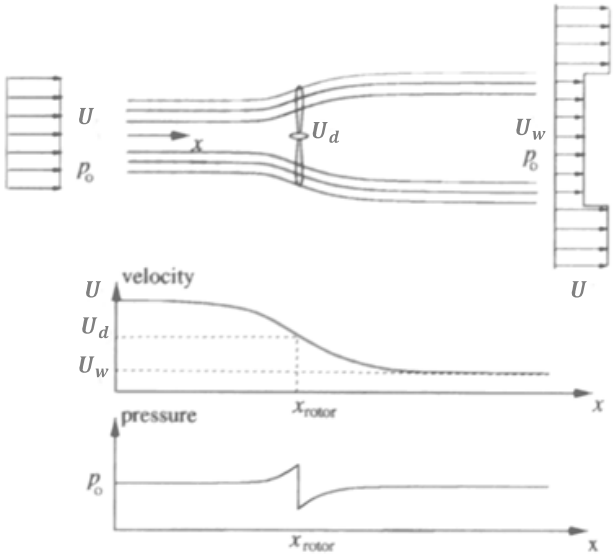

Figure 1 Schematic of the flow through a turbine rotor disc, taken from Hansen, Figure 4.1. U is the upstream flow, U_d is the flow through the rotor disc and U_W is the flow in the fully-expanded wake.

The quantity used to describe the strength of the wind speed deficit in the wake relative to the upstream flow is called the Axial Induction Factor a, which is defined as follows:

$$U_d = (1 - a)U \quad (1)$$

U_d is the axial flow speed through the rotor disc (m/s) and U is the upstream wind speed (m/s).

The 1-D momentum theory discussed above, together with (1), leads to a relationship between U and the axial flow speed in the fully expanded wake U_w (see Hansen Chapter 4 for the full derivation):

$$U_w = (1 - 2a)U \quad (2)$$

In other words, the maximum wind speed deficit in the wake ΔU_{max} is $2aU$.

The wake is modelled in ADMS as an effective volume source with square cross-section representing the fully-expanded wake where the axial flow speed is U_W. The cross-sectional area of the source is equal to the cross-sectional area of the expanded wake. This type of source has an initial 'top-hat' vertical and horizontal profile, which decays to a Gaussian-shape profile as it evolves downstream (see Figure 3). Figure 2 shows a schematic of the expanding stream-tube and the ADMS volume source.

The justification for using a square cross-section volume source rather than a circular one is mainly pragmatic; circular cross-section volume sources are not standard in ADMS and implementing this new source type, or building a circular composite source from many volume sources, is unlikely to yield much benefit due to the evolution of the profile to a Gaussian shape within a few source diameters.

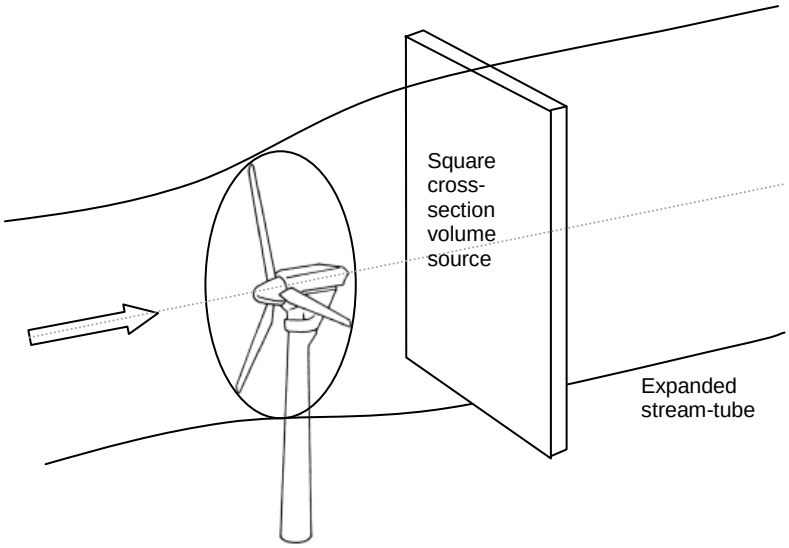

Figure 2 Schematic of the expanding stream-tube of air flowing through the turbine rotor, and the ADMS volume source representing that turbine.

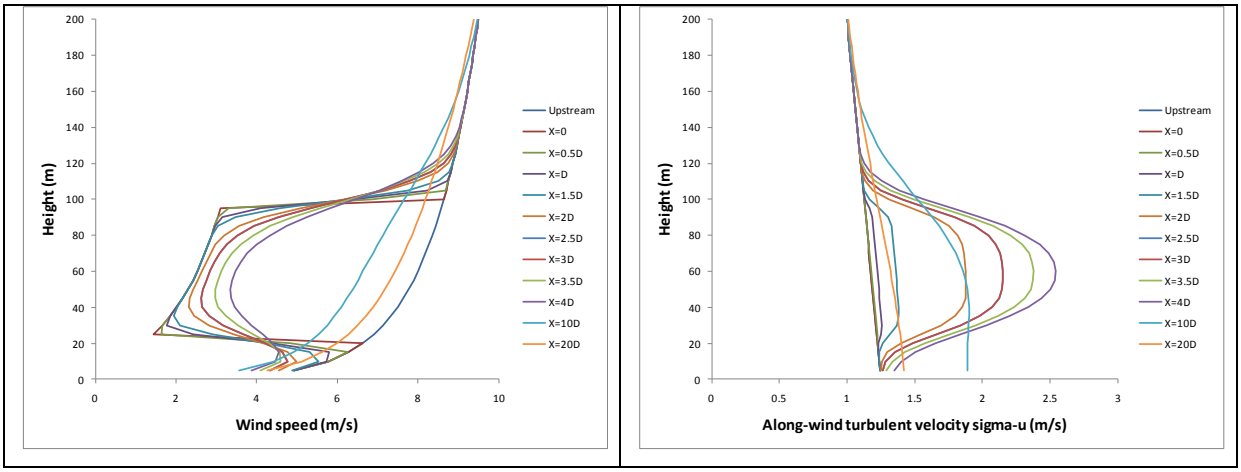

Figure 3 Demonstration of how the vertical profiles of total wind speed and along-wind turbulent velocity develop downwind of the source using the ADMS model (this example is for Tjæreborg 60m turbine, upstream flow 8m/s, see section 4.1 for more details)

To calculate the dimensions of the volume source we use classical 1-D momentum theory again:

$$U_d \times A_d = U_w \times A_w \tag{3}$$

$A_d = \pi\left(\frac{D}{2}\right)^2$ is the area of the rotor disc, D is the diameter of the rotor, $A_w = dy^2$ is the cross-sectional area of the fully-expanded wake and dy is the crosswind extent of the ADMS volume source (which being square, is equal to the vertical extent).

Putting (2) into (3) gives

$$(1-a)U \times \pi\left(\frac{D}{2}\right)^2 = (1-2a)U \times dy^2$$

This reduces to

$$dy = \frac{D}{2}\sqrt{\frac{\pi(1-a)}{(1-2a)}} \tag{4}$$

To keep complications to a minimum, ADMS assumes zero yaw, which is fair in the case of most modern turbines, which have efficient mechanisms to bring the turbine rotor disc perpendicular to the inflow wind as quickly as possible. The ADMS volume source is therefore always perpendicular to the upstream flow. The along-wind extent of the volume source is always 1m. The volume source vertices are set automatically; the user enters only the coordinates of the turbine centre.

The turbine effective source strength is calculated inversely from the known maximum wind speed deficit $\Delta U_{max} = 2aU_\infty$. In model terms, with ΔU as a surrogate for concentration, ΔU_{max} can be expressed as

$$\Delta U_{max} = \frac{Q \times V_{src}}{\dot{V}} \tag{5}$$

Q is the source strength (in units of ms^{-2}), V_{src} is the source volume, and $\dot{V}$ is the volume flow rate through the source. Rearranging (5) gives

$$Q = \frac{\Delta U_{max} \times \dot{V}}{V_{src}} = \frac{2aU \times dy^2 \times U}{1 \times dy^2} = 2aU^2$$

To summarise, the turbine effective source parameters calculated by the model from the upstream flow are as follows:

1. Source dimensions: $dy = dz = \frac{D}{2}\sqrt{\frac{\pi(1-a)}{(1-2a)}}$
2. Source strength: $Q = 2aU^2$

These parameters are all functions of the Axial Induction Factor a, which must in turn be calculated from information about the turbine itself.

3.1.2 Calculation of the Axial Induction Factor

ADMS includes two options for the calculation of the axial induction factor, allowing the modeller to choose the option best suited to the turbine data available:

1) Iterative solution of the Blade Element Momentum (BEM) theory equations; requires
   a) Pitch angle as a function of wind speed
   b) Lift coefficient as a function of the inflow angle of attack
   c) Drag coefficient as a function of the inflow angle of attack
   d) Blade chord length as a function of radial distance from turbine hub
   e) Blade twist angle as a function of radial distance from turbine hub
   f) Number of turbine blades
   g) Angular velocity of the rotor blades

2) Calculation from the thrust coefficient C_T; requires
   a) Thrust coefficient as a function of wind speed (either measured or calculated)

Both methods also require the power coefficient C_p as a function of wind speed in order to calculate power deficits at turbines within other turbine wakes.

This section describes the implementation of each of the above options.

3.1.2.1 Iterative solution of the Blade Element Momentum (BEM) equations

Blade Element Momentum (BEM) theory is the extension of the classical 1-D momentum theory to include the behaviour of the flow close to the actual blades. Instead of treating the turbine as a uniform rotor disc, it splits it up into a series of annuli, so that the 'stream-tube' from the 1-D theory becomes a series of tubes with radius r and wall width dr. The following assumptions are made:

- Annuli are independent of each other
- The force on the flow from the blades is constant in each annular element, i.e. assumes an infinite number of blades

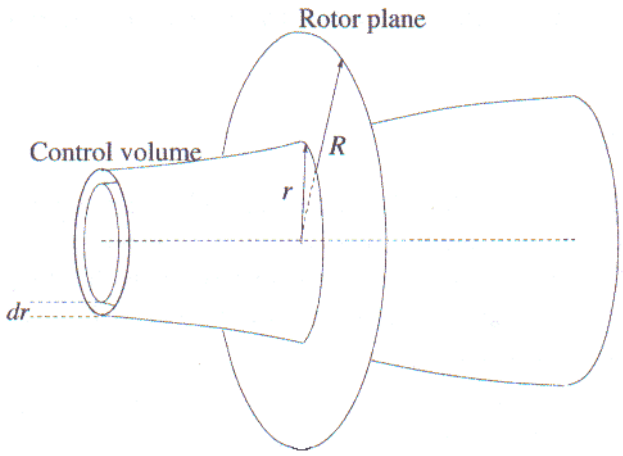

Figure 4 Schematic of the splitting up of the stream tube into annular elements (taken from Hansen, Fig 6.1)

For the full derivation of the BEM theory equations, the reader is referred to Hansen Chapter 6; here only the equations relevant to the calculation of a are given.

The relative velocity seen by the turbine blade is a combination of the axial velocity $(1-a)U$ and the induced tangential velocity $(1+a')\omega r$ where ω is the angular velocity of the rotor and a' is the 'Tangential Induction Factor'.

ϕ is the angle between the relative velocity and the rotor plane, and is therefore the sum of the local 'pitch' of the blade θ and the 'angle of attack' α:

$$\phi = \theta + \alpha$$

$$tan\phi = \frac{(1-a)U}{(1+a')\omega r}$$

C_{norm} and C_{tang} are the components of the 'Lift' (force perpendicular to the velocity seen by the aerofoil) and the 'Drag' (force parallel to the velocity seen by the aerofoil) in the axial and tangential directions respectively:

$$C_{norm} = C_l cos\phi + C_d sin\phi$$

$$C_{tang} = C_l sin\phi - C_d cos\phi$$

C_l and C_d are the lift and drag coefficients respectively (these are functions of the angle of attack α).

$\sigma(r)$ is the 'blade solidity', defined as the fraction of the annular area covered by blades:

$$\sigma(r) = \frac{c(r)B}{2\pi r}$$

$c(r)$ is the local 'chord length' of the blade and B is the number of blades.

The governing equations of BEM theory are then:

$$a = \frac{1}{\frac{4sin^2\phi}{\sigma C_{norm}} + 1}$$

$$a' = \frac{1}{\frac{4sin\phi cos\phi}{\sigma C_{tang}} - 1}$$

The equations for a and a' have to be solved iteratively, due to the inter-dependence of a, a' and ϕ. The iteration starts with $a = a' = 0$.

The final value of a used to calculate the effective source parameters is the weighted average of the values calculated from the blade root to the blade tip. This value is limited to being no greater than 0.49, to prevent negative flow.

3.1.2.1.1 Corrections that must be applied to BEM theory

In order to deal with some of the physical limitations of classical BEM theory, two corrections are applied to the governing equations; these are described in this section.

Prandtl's Tip Loss Factor

The BEM theory assumes that there are an infinite number of blades. Prandtl's Tip Loss Factor corrects this assumption.

The equation for Prandtl's Tip Loss Factor F is

$$F(r) = \frac{2}{\pi} cos^{-1}\left(e^{-f(r)}\right)$$

$$f(r) = \frac{B}{2}\frac{(R-r)}{rsin\phi}$$

Applying this factor results in modified equations for a and a':

$$a = \frac{1}{\frac{4Fsin^2\phi}{\sigma C_x} + 1}$$

$$a' = \frac{1}{\frac{4Fsin\phi cos\phi}{\sigma C_y} - 1}$$

Corrections for high values of a

The BEM theory has a problem for high values of a because of the relationship $U_w = (1-2a)U$, which cannot apply for a greater than 0.5, because this implies that the flow reverses direction, which we know not to be the case; instead, physically, the flow becomes very turbulent and entrains outside air, i.e. the stream-tube breaks down and classical momentum theory alone no longer holds.

In the standard case where momentum theory holds, the thrust coefficient C_T is defined so that

$$C_T = 4a(1-a)F$$

In order to correctly predict the thrust when a is high, Wilson and Walker proposed a correction:

$$C_T = \begin{cases} 4a(1-a)F & a \le a_c \\ 4({a_c}^2 + (1-2a_c)a)F & a > a_c \end{cases}$$

where $a_c \approx 0.2$.

This new formulation for C_T affects the calculation of a as follows.

$$a = \begin{cases} \dfrac{1}{\mathrm{K}+1} & a \le a_c \\ \dfrac{1}{2}\left[2 + K(1-2a_c) - \sqrt{(K(1-2a_c)+2)^2 + 4(Ka_c{}^2 - 1)}\right] & a > a_c \end{cases}$$

$$K = \frac{4Fsin^2\phi}{\sigma C_{norm}}$$

The calculation of a' is unchanged.

3.1.2.2 Calculation from the thrust coefficient

The main drawback of the above method of calculating the axial induction factor a is the amount of turbine data required to carry out the calculations. Only in rare cases are the full data available for a particular turbine.

However, the variation of the turbine's thrust coefficient with wind speed does seem to be more readily available, either measured or calculated by the turbine manufacturer from BEM theory using the full turbine data.

The standard relationship between thrust coefficient C_T and a is

$$C_T = 4a(1-a)$$

However, as discussed above, this breaks down as the flow in the wake becomes turbulent for high values of a, so Wilson and Walker proposed a correction:

$$C_T = \begin{cases} 4a(1-a)F & a \le a_c \\ 4(a_c{}^2 + (1-2a_c)a)F & a > a_c \end{cases}$$

where $a_c \approx 0.2$.

This becomes an equation for a in terms of C_T:

$$a = \begin{cases} \dfrac{1}{2}\left(1 - \sqrt{1-C_T}\right) & C_T \le 0.64 \\ \dfrac{C_T - 4a_c{}^2}{4(1-2a_c)} & C_T > 0.64 \end{cases}$$

3.1.3 Special dispersion characteristics of wind turbine wakes

The previous section described the calculation of the turbine effective volume source parameters from the upstream flow and from the turbine data. This section discusses some areas where it has been identified that a turbine wake disperses differently to a plume of material and it describes the corresponding developments made to ADMS to account for these differences.

3.1.3.1 Velocity fluctuations

The ADMS fluctuations model is applied to simulate the meandering-induced turbulence, with concentration fluctuations acting as a surrogate for velocity fluctuations. However, the standard ADMS fluctuations model calculates components of fluctuations due to three plume characteristics, shown in Figure 6.

The components due to plume meandering and entrainment of ambient air into the plume are applicable to wind turbine wake modelling, but 'in-plume turbulent mixing' has no equivalent meaning for wind turbine wake modelling, so this component is ignored.

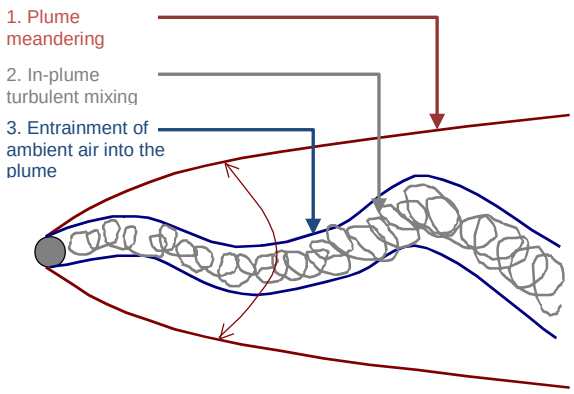

Figure 5 Schematic diagram of the contributing factors to concentration fluctuations in the standard ADMS fluctuations model.

3.1.3.2 Entrainment of ambient air into the wake

As part of the TOPFARM project, researchers at DTU in Denmark who are doing CFD modelling of the wakes behind wind turbines have analysed the effect of inflow turbulence on the stability of the vortex tube generated by the tip vortices from the rotating blade tips. The pictures in Figure 6 show the vorticity on a horizontal cross section through the centres of three turbines aligned with the wind direction (represented by the black lines). Wind flow is from left to right. The top picture has a stable inflow, i.e. no initial turbulence; the bottom picture has a turbulent inflow.

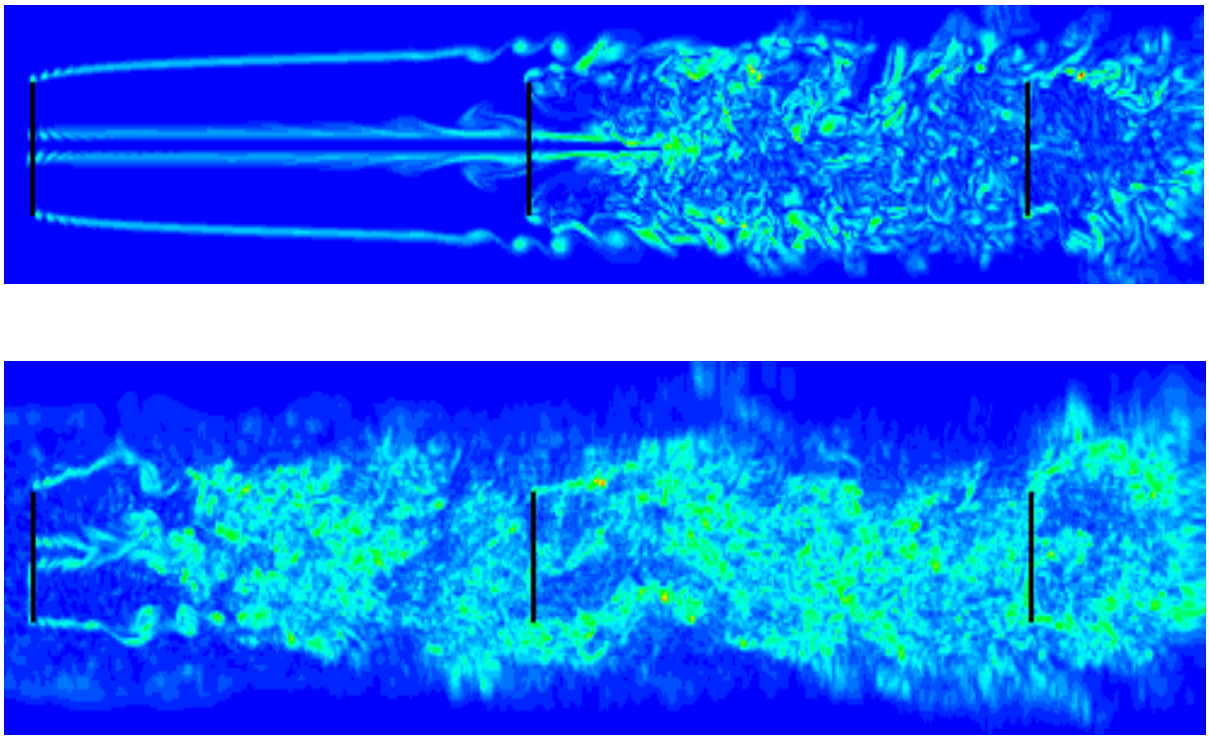

Figure 6 Development of the wake behind three rotors in a row with U=10m/s; Turbine spacing 3D; stable inflow (top), turbulent inflow (bottom). Picture from CFD modelling done by Jens Sørensen and colleagues at DTU, Denmark (partners in TOPFARM).

From the pictures in Figure 6 we can see how with a stable inflow the vortex tube is slow to break down, but with a turbulent inflow the breakdown occurs rapidly. The picture also demonstrates how the vortex tube downwind of the turbines inside the wake of upstream turbines breaks down immediately, even when there is no turbulence in the upstream flow.

This effect has been incorporated into ADMS simply by delaying the point downwind of the turbine at which the wake starts to entrain air, and by making this delay dependent on the ambient turbulence levels. In addition, if a turbine lies inside the wake of an upstream turbine then no delay is imposed; the wake entrains ambient air immediately.

Entrainment of ambient air into a plume is inherently modelled in two ways in ADMS: in the normal calculation of plume spread in the dispersion code, and also in the fluctuations calculations. This means that any change to simulate a delay in the entrainment of the air into a wind turbine wake must be done both in the dispersion code and also in the fluctuations calculations.

The ADMS model fluctuations technical specification document P13/07, page 10, equation (22), describes how σ_Δ, the plume spread due to entrainment, is calculated:

$$\sigma_\Delta^2 = \frac{\sigma_1^2 R^2}{\sigma_1^2 + A_0 \sigma_1 R + R^2}$$

where σ_1 is the standard plume spread, $R = \varepsilon t^3/3$, ε is the dissipation rate, t is the time since release and A_0 is a tuneable constant lying in the range (0,2) (=0.2 in the current ADMS code).

To delay the effect of entrainment on the plume spread, two changes have been made:

1. In the fluctuations code, the calculation of R^2 has been modified so that the value of t used is reduced by t_E to account for the entrainment delay. In other words, $\sigma_\Delta = 0$ for $t < t_E$.
2. In the main dispersion code, the entrainment component of plume spread is calculated, with and without delay, and the difference removed from the total plume spread.

The expression for t_E is

$$t_E = t_{u_{min}} + 3 \times \frac{D}{U} \times \exp\left(-20 \times \max(I - 0.05, 0)\right)$$

where $t_{u_{min}} = \frac{2D}{U}$, D is the turbine diameter (m), U is the ambient wind speed at the hub height (m/s) and I is the ambient turbulence intensity (dimensionless), defined as

$$I = \frac{\sqrt{\frac{1}{3}({\sigma_u}^2 + {\sigma_v}^2 + {\sigma_w}^2)}}{U}$$

If the centre of the turbine lies inside the wake of an upstream turbine then $t_E = 0$.

3.1.3.3 Shear-induced turbulence

At the edge of a turbine wake, there is a gradient in the speed of the air flow, which generates turbulence in the wake that is not included in the standard ADMS model. An extra component of turbulence σ_{shear}, has been added to account for this.

Bevilaqua and Lykoudis (1978), proposed that the relationship between maximum wind speed deficit ΔU_{max}, upstream wind speed U and shear-induced turbulent velocity u' is

$$\Delta U_{max} \sim -0.65U$$

$$u'/U \sim 0.06$$

$$\frac{u'}{\Delta U_{max}} \sim 0.1$$

For this reason, for turbines not in the wake of any other turbines, σ_{shear} is calculated in ADMS as

$$\sigma_{shear} = \begin{cases} 0.1|\Delta U_{max}| & 7D \leq x \\ \left(\frac{x-2D}{5D}\right) 0.1|\Delta U_{max}| & 2D \leq x \leq 7D \\ 0 & x \leq 2D \end{cases}$$

D is the diameter of the turbine, x is the downwind distance from the (effective) source, ΔU_{max} is the maximum wind speed deficit.

For turbines that are inside the wake of another turbine, the initial growth of the turbulence is skipped, and $\sigma_{shear} = 0.1|\Delta U_{max}|$ is applied at all downstream distances.

3.1.3.4 Large-scale meandering

The standard ADMS model includes a component of horizontal plume spread due to large scale wind direction meandering. Observations suggest that this large scale meandering is reduced in a wind farm environment and that this meandering is on a scale much larger than the wind turbines themselves, so this component of plume spread is ignored when modelling wind turbine wakes.

3.2 Multiple turbines

In standard ADMS, in the absence of plume chemistry, the plume due to one source does not affect any other source or plume, and the concentration field due to multiple sources is the sum of the concentration field due to each source.

In the case of wind turbine wake modelling, the wake downwind of a turbine affects all downwind turbines. For this reason, developments have been made to ADMS in order to properly account for the effect of the change in the wind field due to upstream turbines on downstream turbines. This section describes these changes.

3.2.1 Ordering of sources

Before the dispersion calculations are carried out for each input meteorological condition, all the input turbine sources are re-ordered according to their downwind position; the most upstream turbine source is modelled first, the most downstream turbine source is modelled last. The assumption is made that turbines are only affected by the wakes from *upstream* turbines.

3.2.2 Modification to wind speed and turbulence profiles

The vertical profile of wind speed and turbulence used in ADMS is modified for each turbine to include the effect of the wakes from all upstream turbines, which is made possible by the ordering of turbine sources described above. Wind and turbulence is assumed to be spatially uniform in the dispersion of each wake.

At the location of each turbine, at a range of heights within the atmospheric boundary layer, the values of U and along-wind component of turbulent velocity σ_U are adjusted from the standard upstream ADMS profile to include the wind speed deficit and the meandering-induced σ_U respectively at that point. This change in the wind and turbulence profile for each turbine in a wind farm affects the characterisation of the effective volume source and the amount of entrainment delay imposed, as well as the dispersion of the wake.

3.2.3 Turbines inside the wakes of upstream turbines

Some aspects of the dispersion of turbine wakes are different if the turbine is inside the wake of an upstream turbine; namely the delay in entrainment (see section 3.1.3.1), and shear-induced turbulence (see section 3.1.3.3). The method adopted for determining if a turbine is inside the wake of an upstream turbine is as follows:

> If turbine B is downwind of turbine A, then turbine B is identified as being inside the wake of turbine A if the crosswind distance from the centre of turbine A to the centre of turbine B is less than half the width of the volume source representing turbine A plus $2\sigma_y$, where σ_y is the lateral horizontal plume spread in turbine A's wake at the same downwind distance as turbine B.

4. Validation

The performance of the ADMS wake model has been tested against a number of datasets of turbine measurements, including both single turbine data and wind farm data. This section describes these datasets, the model setup used in the simulations and compares model results with measurements in each case.

In all cases, site data, turbine data and measurements have been kindly provided by Kurt Hansen from DTU, Denmark.

The method selected for calculating the Axial Induction Factor in ADMS is the thrust coefficient (C_T) method in all cases except the Tjæreborg 60m/2MW turbine, where results have been obtained using both the thrust coefficient (C_T) method and the Blade Elemement Momentum (BEM) theory method.

The definitions of quantities presented in this section are as follows:

$$\text{Normalised wind speed} = \frac{U_{local}}{U_{upstream}}$$

$$\text{Normalised wind speed deficit} = 1 - \frac{U_{local}}{U_{upstream}}$$

$$\text{Total turbulence intensity} = 100 \times \frac{\sqrt{\sigma_{U_{local}}^2 + \sigma_{U_{upstream}}^2}}{U_{upstream}}$$

$$\text{Normalised power} = \frac{P(U_{local})}{P(U_{upstream})}$$

4.1 Tjæreborg 60m/2MW

4.1.1 Site information

Wake measurements have been recorded over a long period of time (1988 to 1993) at a measurement mast 2D downstream of a 60m/2MW test turbine at Tjæreborg Enge wind farm in Esbjerg, Denmark. The diameter of the turbine is 61m; the turbine hub height is 60m.

The wake data available are measurements of normalised wind speed deficit at hub height for 4 flow cases: 6, 8, 10 and 12m/s. The wind direction varies by 40 degrees either side of the case where the measurement mast is directly downstream of the turbine.

The full set of aerodynamic turbine blade data are available for this turbine, as well as calculated thrust coefficient (C_T) data (see Figure 7 and Figure 8). The turbine has 3 blades, and constant rotational speed 2.315 rad/s.

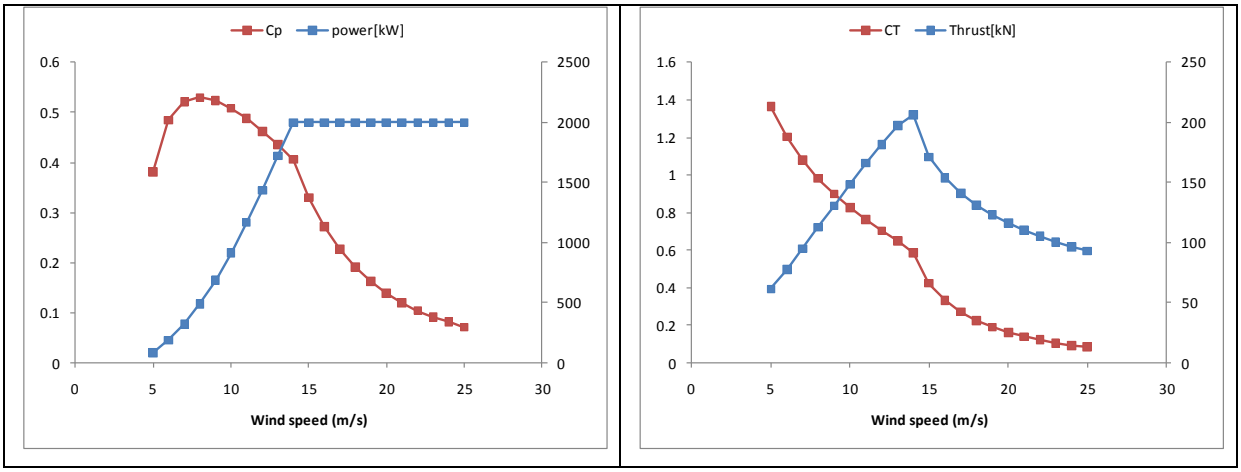

Figure 7 Calculated power (kW), power coefficient C_p, thrust (kN) and thrust coefficient C_T

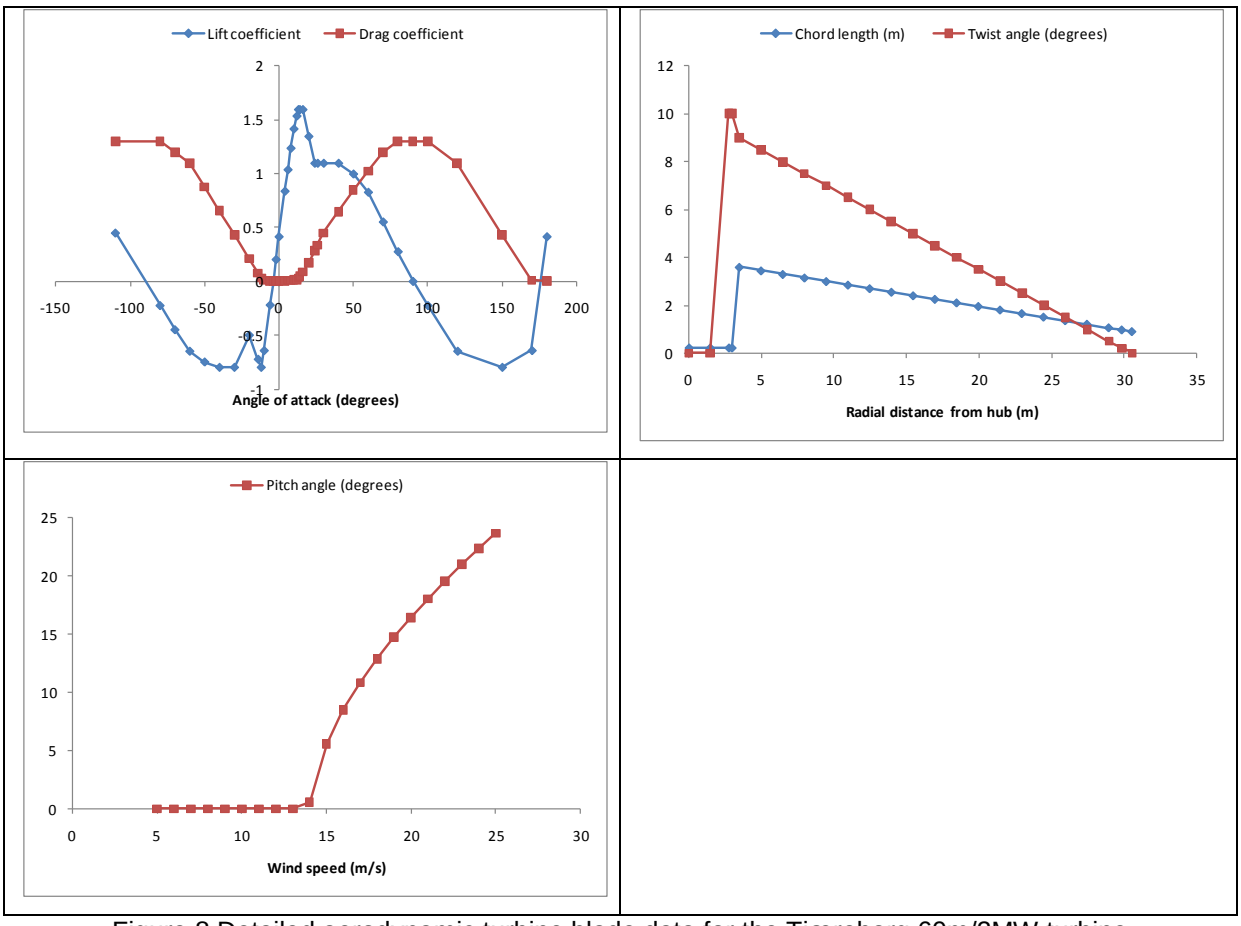

Figure 8 Detailed aerodynamic turbine blade data for the Tjæreborg 60m/2MW turbine

4.1.2 Model setup

The detailed aerodynamic data available for this turbine has made it possible to use the ADMS implementation of the BEM method to calculate the Axial Induction Factor. Calculated thrust coefficient data are also available, so the ADMS simulations have been run twice, once using the BEM method and once using the C_T method; results for both methods are presented in section 4.1.3.

The inputs to ADMS common to both methods were as follows:

- Single source, centre coordinates (0,0)
- Turbine height 60m
- Turbine diameter 61m
- C_p as a function of wind speed (see Figure 7)
- Single output receptor directly east of the source, coordinates (122,0)
- 4 flow cases: U=6, 8, 10 and 12m/s
- For each flow case, wind directions modelled from 230 to 310 degrees inclusive, in 5 degree intervals
- Boundary layer height 800m, ground heat flux 0W/m^2, i.e. neutral conditions
- Surface roughness 0.1m

For the BEM method, the following data were also input (see Figure 8):

- Lift coefficient C_L and drag coefficient C_D as a function of inflow angle of attack
- Chord length (m) and blade twist angle (degrees) as a function of radial distance from hub
- Pitch angle (degrees) as a function of wind speed

For the C_T method, C_T as a function of wind speed was also input (see Figure 7).

4.1.3 Results

The model results agree well with measured data for the U=8m/s, the model under-predicts the deficit for U=10m/s and U=12m/s and over-predicts the deficit for U=6m/s.

The measured data shows a maximum normalised wind speed deficit of around 0.7 for all flow cases, while the wake becomes narrower as the upstream wind speed increases. The model results however, for both BEM and C_T methods, demonstrate a different behaviour; the wind speed deficit reduces as the inflow wind speed increases. This is due to the fact that the calculated axial induction factor reduces as the wind speed increases (see Table 1).

The calculated values of the axial induction factor in Table 1 also explain the differences between the modelled results for the BEM and C_T methods; the C_T method yields lower values of the axial induction factor and hence lower wake deficits.

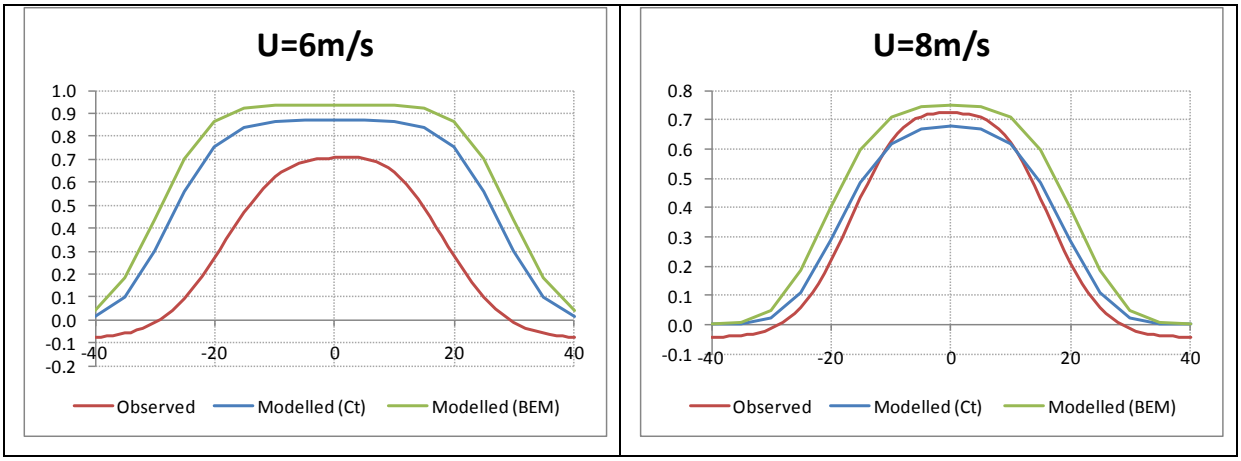

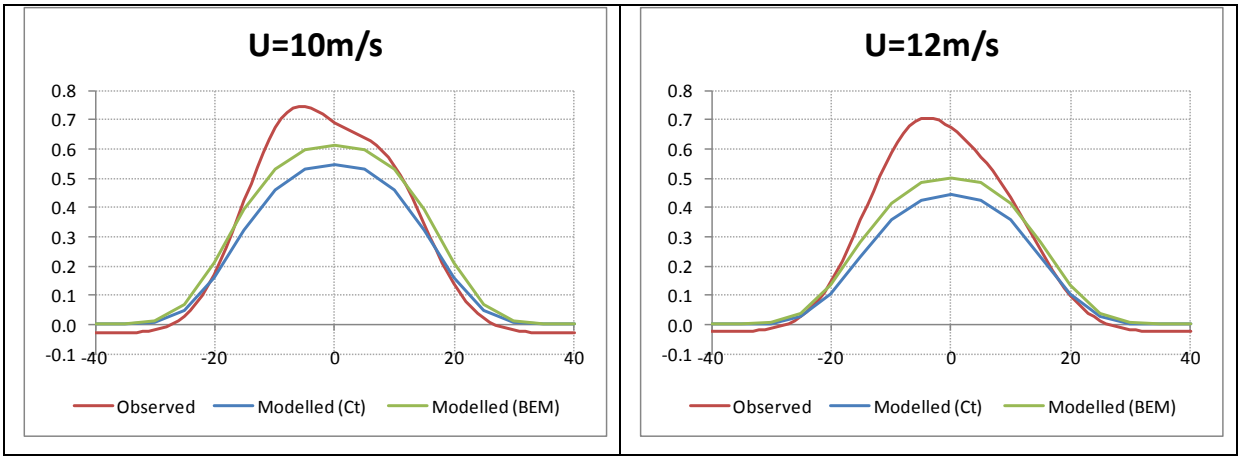

Figure 9 Comparison of modelled and observed normalised wind speed deficit at the hub height (60m) at a receptor which is 2D downstream when the wind direction is 0 degrees.

Upstream wind speed	BEM method	C_T method
6m/s	0.46925	0.43454
8m/s	0.37546	0.34200
10m/s	0.30833	0.27775
12m/s	0.25583	0.22625

Table 1 Calculated values of Axial Induction Factor in the 4 flow cases

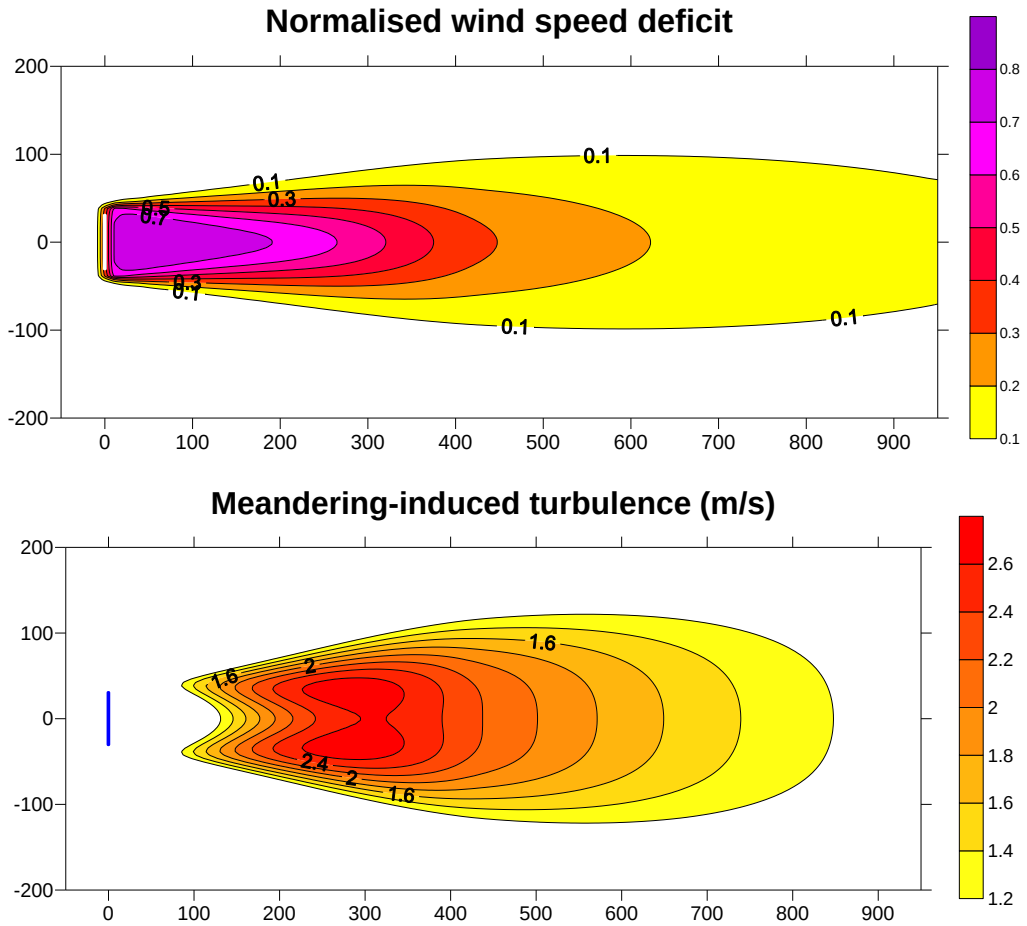

Figure 10 U=8m/s: Contour plots of gridded ADMS output of normalised wind speed deficit and meandering-induced turbulence

4.2 Tjæreborg NM80

4.2.1 Site information

The Tjæreborg NM80 wind turbine is an 80m-diameter 2.5MW turbine located at Tjæreborg Enge wind farm in Denmark. The turbine hub height is 57m. A backward-looking LIDAR was positioned on the turbine hub, giving measurements of wake deficit and total turbulence intensity across the wake 200m (2.5D) downstream.

There are 4 flow cases: FC1 (U=5.2m/s), FC2 (U=7.2m/s), FC3 (U=9.1m/s) and FC4 (U=11.4m/s). In FC4 the turbine's active controller was in use, which affects the wake properties in a way that cannot be simulated by ADMS, so this flow case has not been simulated.

For each flow case there are data relating to the ambient turbulence intensity and the amount of yaw. ADMS assumes zero yaw when characterising the effective turbine source, which should be kept in mind when interpreting the model results.

Little data are available for the NM80 turbine, so power and thrust data have been derived by rescaling data for the NM80/2750kW turbine, for which data are available. The adjusted curves are shown in Figure 11.

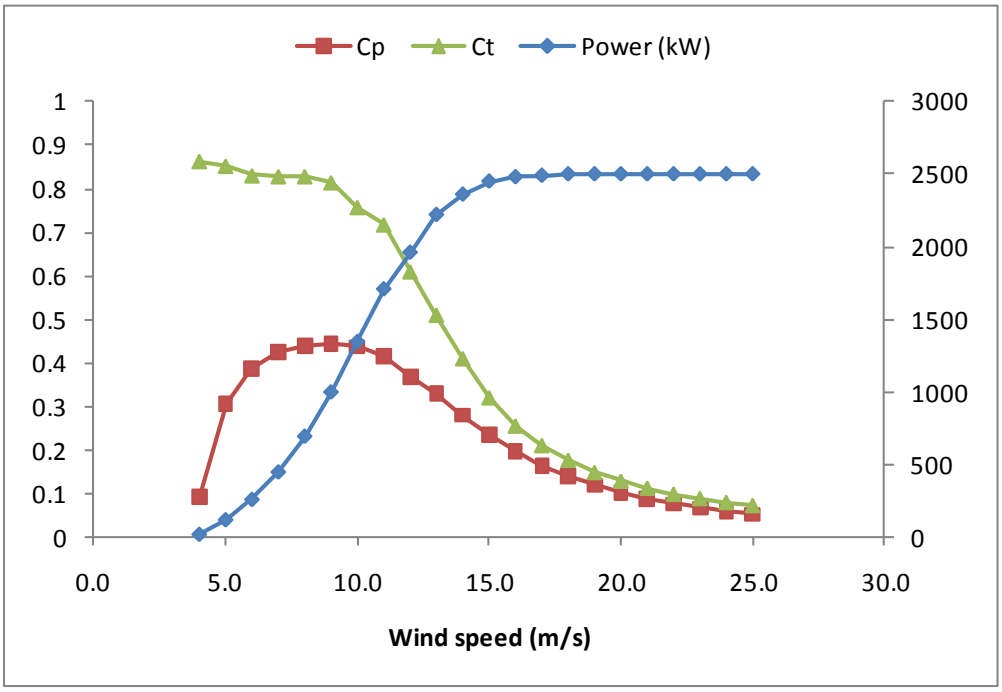

Figure 11 Power output (kW), power coefficient C_p and thrust coefficient C_T as a function of inflow wind speed for the Tjæreborg NM80 turbine

4.2.2 Model setup

Turbulence intensity is not an input to the ADMS model (many different types of atmospheric boundary layer can give the same turbulence intensity at a given height above ground), so each flow case has been simulated with a range of Monin-Obukov values (L_{MO}=-100m, Infinity, 100m) and a range of surface roughness lengths (z_0=0.01m, 0.1m).

The inputs to ADMS were therefore as follows:

- Single source
- Turbine height 57m
- Turbine diameter 80m
- C_p as a function of wind speed (see Figure 11)
- C_T as a function of wind speed (see Figure 11)
- 49 output receptors positioned at 5m intervals 200m directly downwind of the source
- 3 flow cases: U=5.2, 7.2 and 9.1m/s
- 2 surface roughness cases: 0.01m and 0.1m
- 3 L_{MO} cases: -100m, Infinity and 100m

4.2.3 Results

For each flow case, the results presented are normalised wind speed deficit (or 'wake deficit') and total turbulence intensity.

In FC1 (see Figure 12 and Figure 13) the model generally overestimates the wake deficit. The measurements suggest a lower initial wake deficit than calculated by the model, given the turbulence measurements. This may be due to the significant yaw angle in this case (-18 degrees), since ADMS assumes zero yaw.

In FC2 (see Figure 14 and Figure 15) the best agreement between observations and model results is for z_0=0.1m and L_{MO}=100m (stable atmospheric conditions, the green solid lines in the graphs).

In FC3 (see Figure 16 and Figure 17) the best agreement between observations and model results is for z_0=0.01m and L_{MO}=Infinity (neutral atmospheric conditions, the red dotted lines in the graphs).

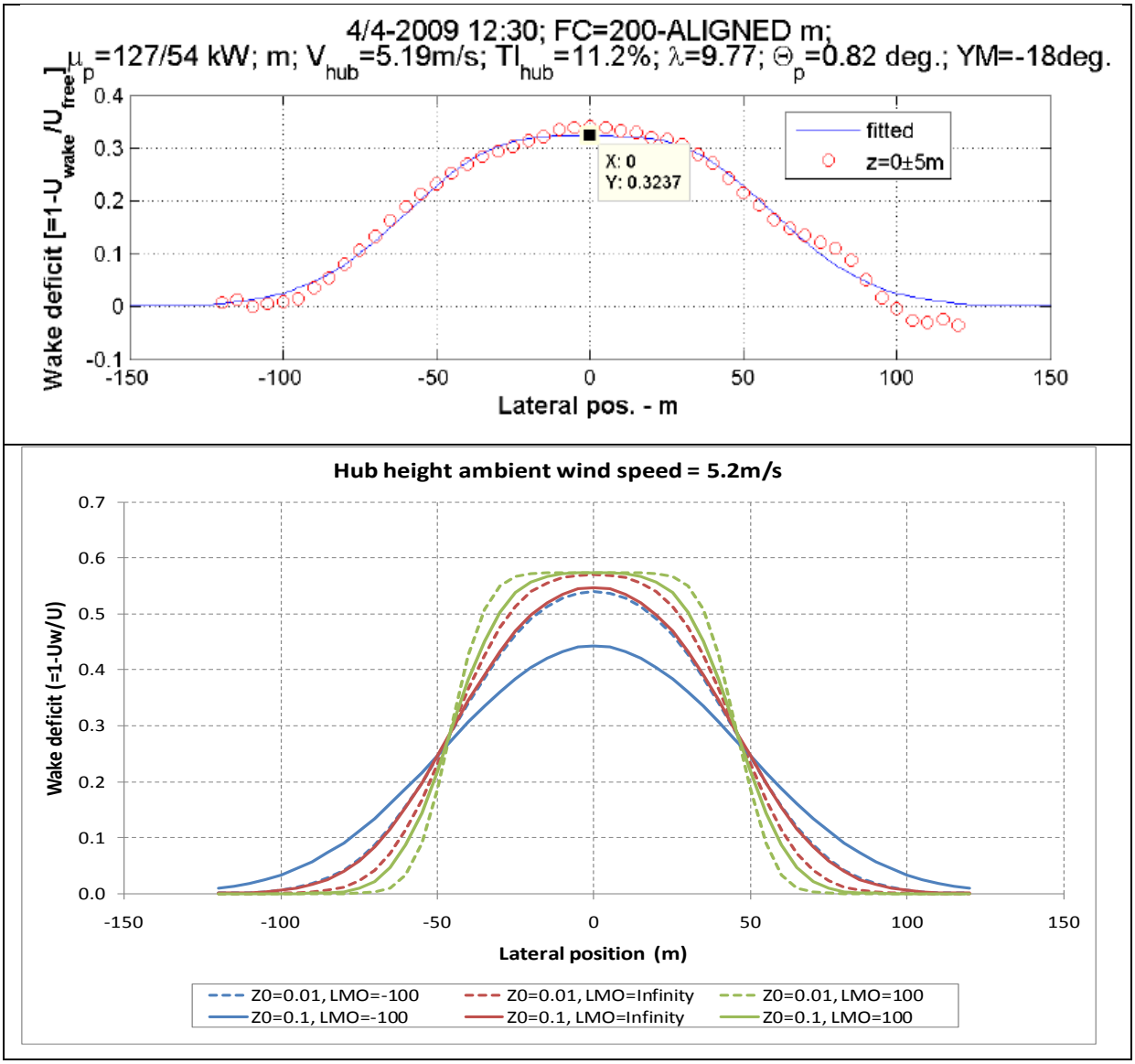

Figure 12 FC1 U=5.2m/s: Observed (top) and modelled (bottom) normalised wind speed deficit at hub height across the wake at 2.5D downstream. Ambient turbulence = 11.2%, yaw=-18 degrees.

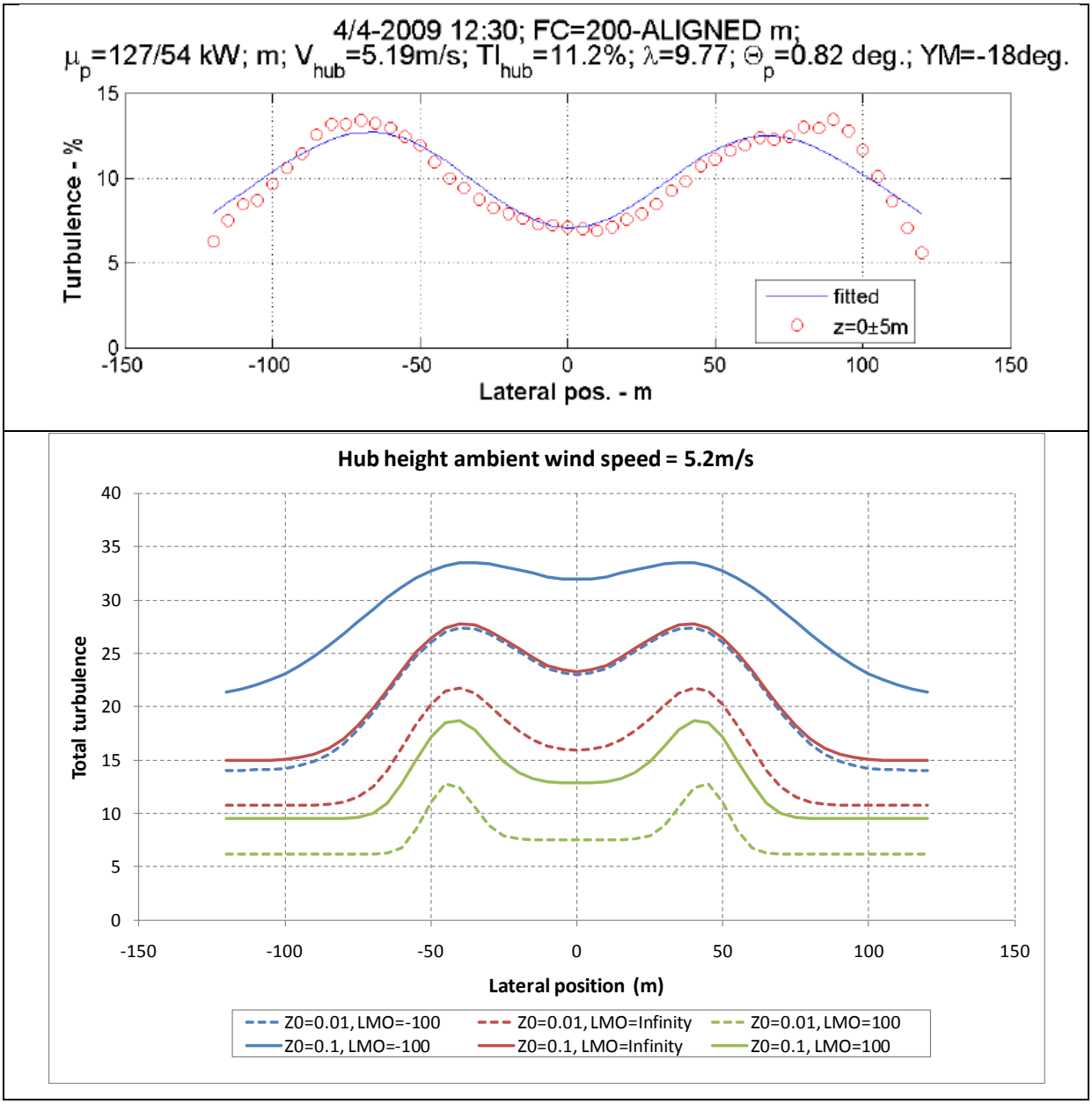

Figure 13 FC1 U=5.2m/s: Observed (top) and modelled (bottom) total turbulence intensity (%) at hub height across the wake at 2.5D downstream. Ambient turbulence = 11.2%, yaw=-18 degrees.

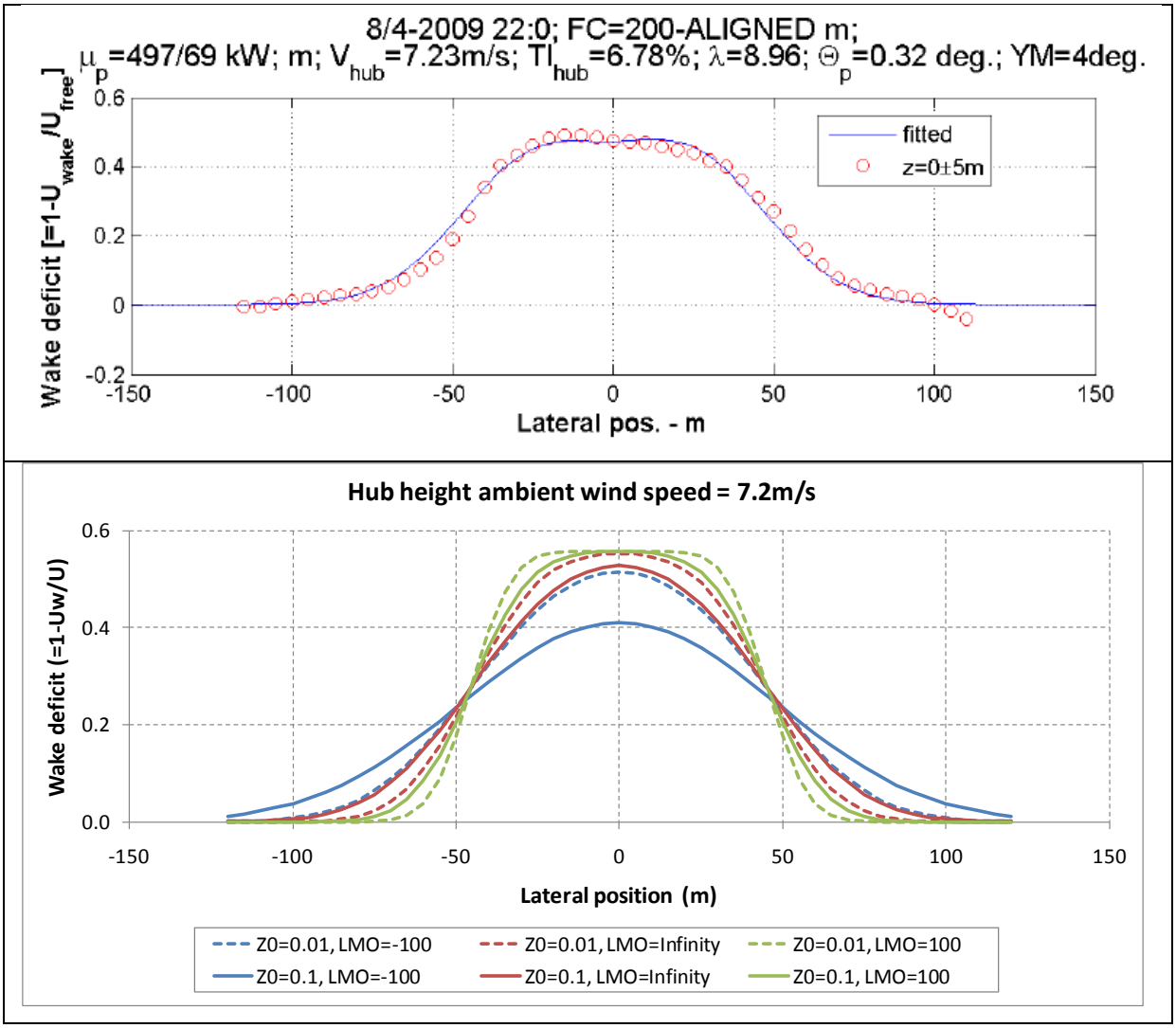

Figure 14 FC2 U=7.2m/s: Observed (top) and modelled (bottom) normalised wind speed deficit at hub height across the wake at 2.5D downstream. Ambient turbulence = 6.78%, yaw=4 degrees.

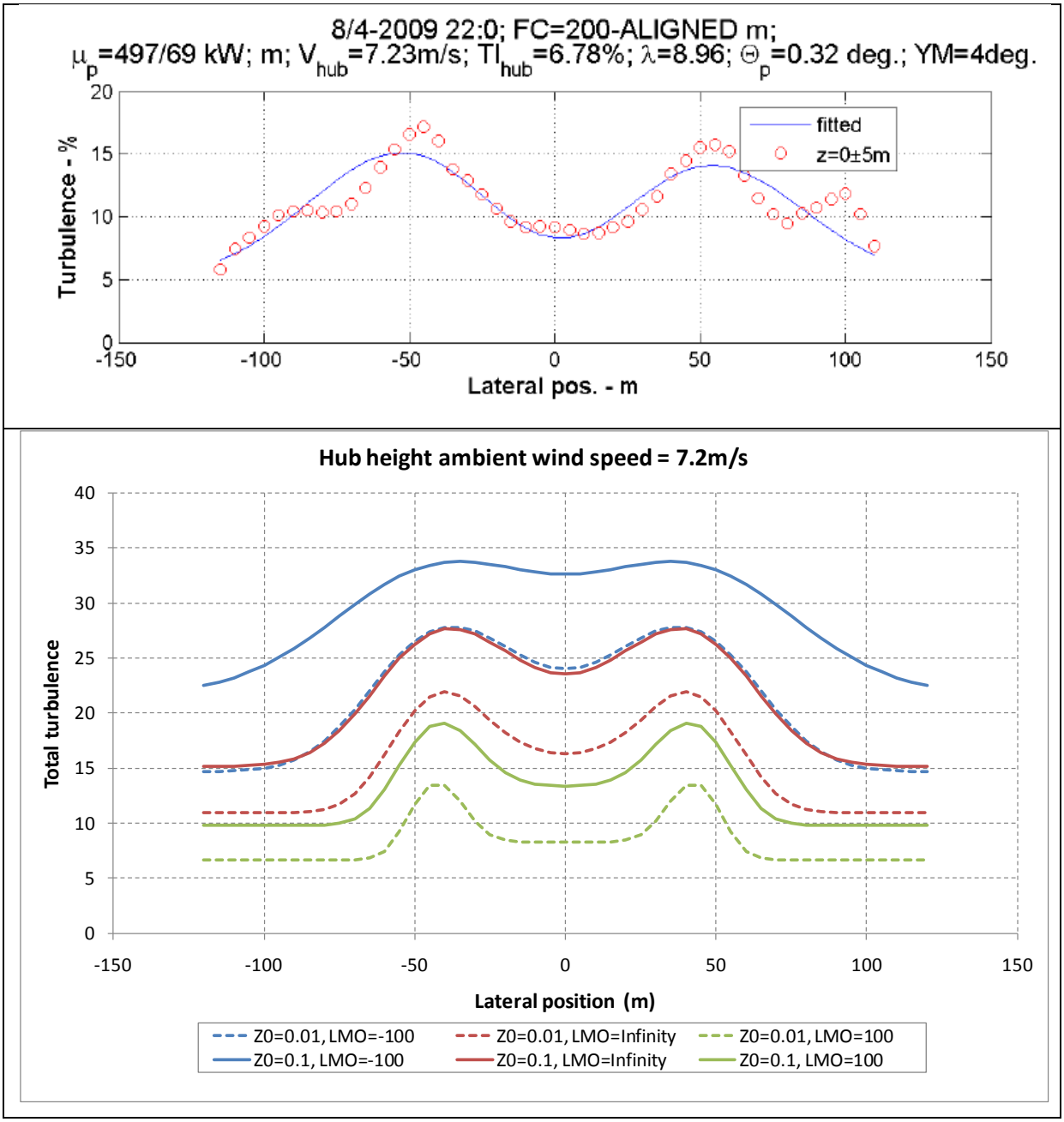

Figure 15 FC2 U=7.2m/s: Observed (top) and modelled (bottom) total turbulence intensity (%) at hub height across the wake at 2.5D downstream. Ambient turbulence = 6.78%, yaw=4 degrees.

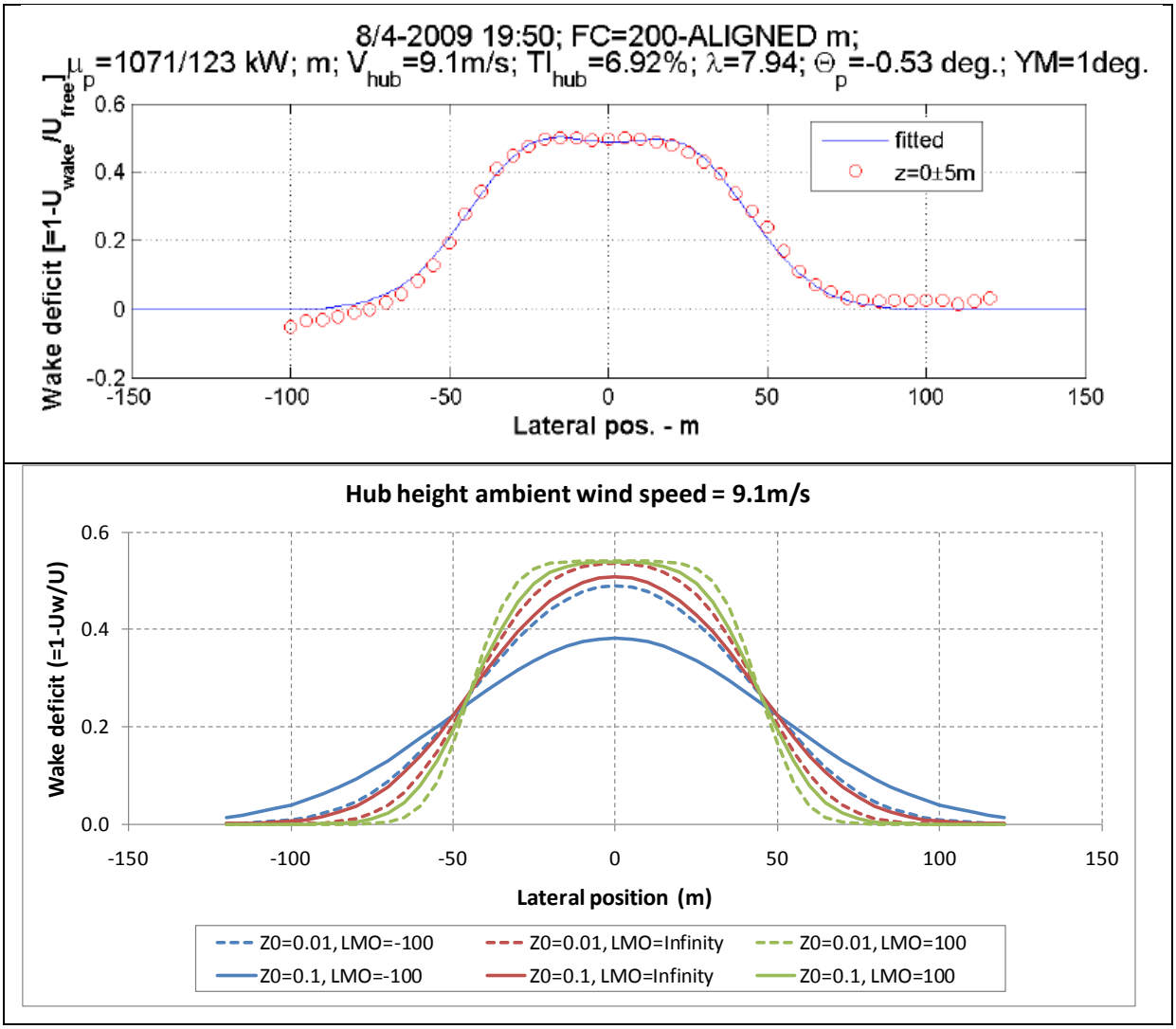

Figure 16 FC3 U=9.1m/s: Observed (top) and modelled (bottom) normalised wind speed deficit at hub height across the wake at 2.5D downstream. Ambient turbulence = 6.92%, yaw=1 degree.

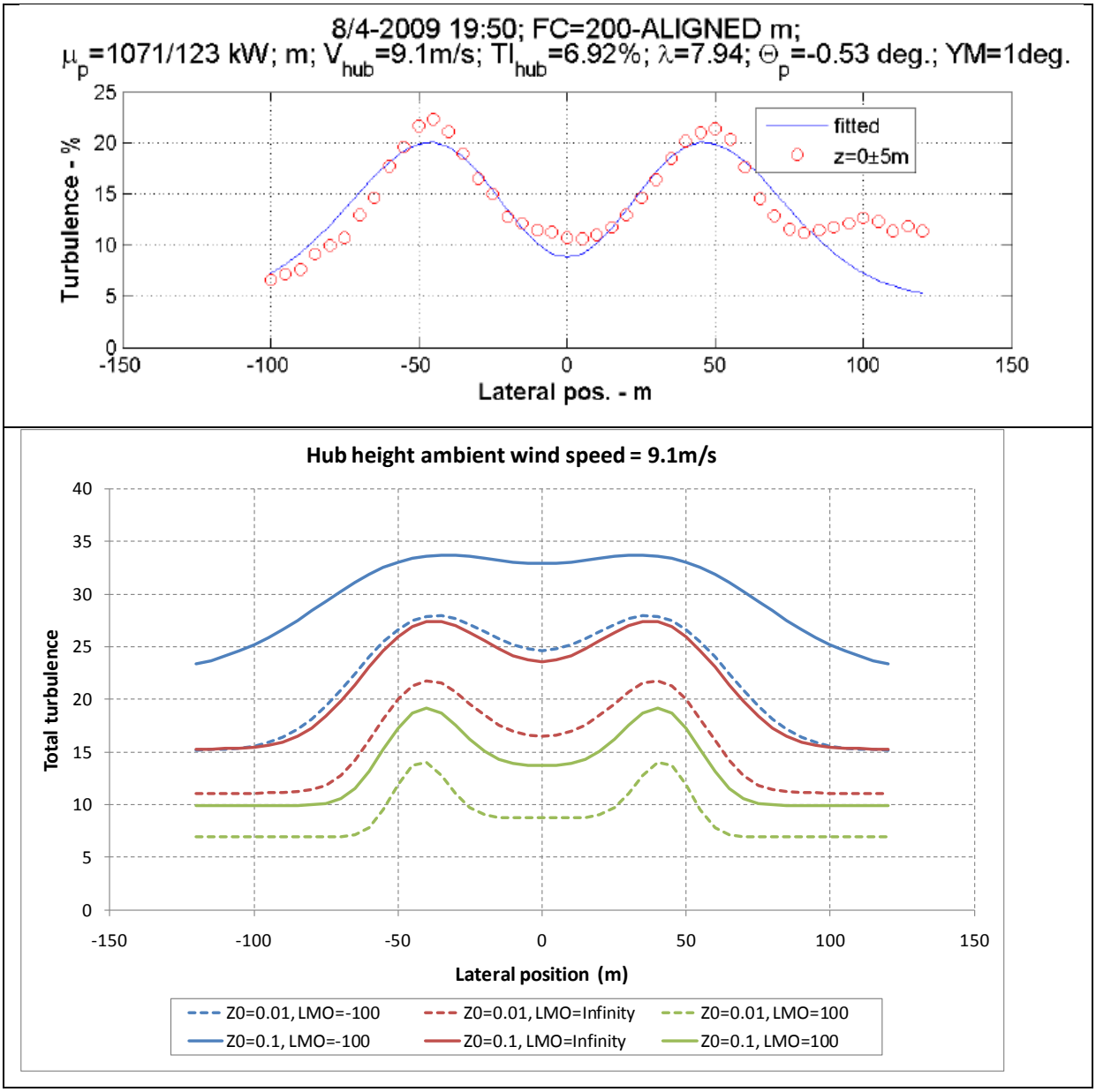

Figure 17 FC3 U=9.1m/s: Observed (top) and modelled (bottom) total turbulence intensity (%) at hub height across the wake at 2.5D downstream. Ambient turbulence = 6.92%, yaw=1 degree.

4.3 Nysted wind farm

4.3.1 Site information

Nysted wind farm consists of 72 turbines arranged in a parallelogram grid with 8 columns and 9 rows, with the rows at an angle of 8° to the W-E direction. The layout of the turbines is shown in Figure 19, along with the 7 wind direction cases for which measurements are available: 263, 268, 273, 278, 283, 288 and 293 degrees. There are 3 wind speed cases: 6, 8 and 10m/s.

Each turbine is a Bonus 2.3MW turbine, with diameter 82.4m and height 69m.

The measurements available are normalised power at every turbine for each wind speed and direction case, with reference to the power generated at turbine A05, in the middle of the upstream column.

Figure 18 Map showing the location of the Nysted wind farm off the coast of Denmark

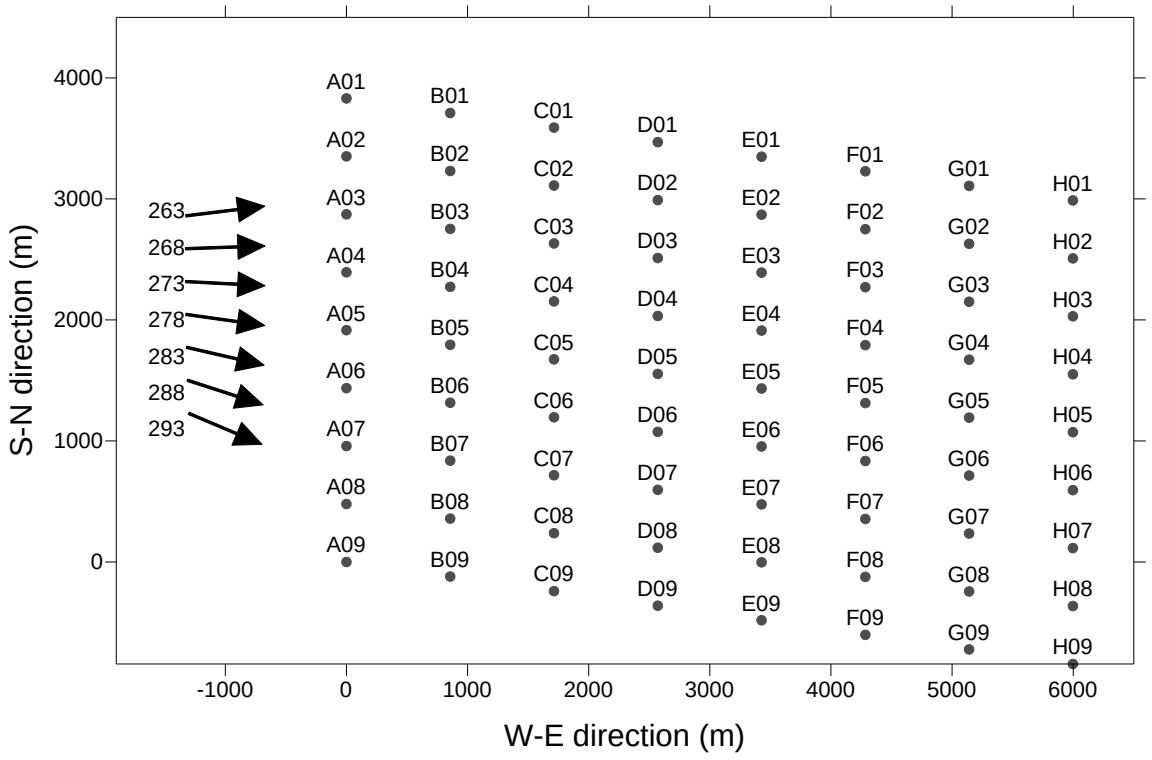

Figure 19 Layout of turbines in the Nysted wind farm

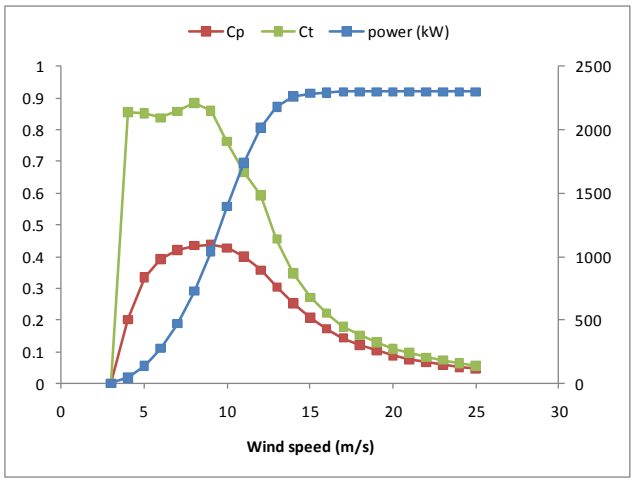

Figure 20 Power output (kW), power coefficient C_p and thrust coefficient C_T as a function of inflow wind speed for the Bonus 2.3MW turbines installed at the Nysted wind farm.

4.3.2 Model setup

The inputs to ADMS were as follows:

- 72 turbine sources (9 rows, 8 columns), locations as shown in Figure 19
- Turbine height 69m
- Turbine diameter 82.4m
- C_p as a function of wind speed (see Figure 20)
- C_T as a function of wind speed (see Figure 20)
- Output receptors at each turbine location at hub height
- 3 flow cases: U=6, 8 and 10m/s
- 7 wind direction cases: 263, 268, 273, 278, 283, 288 and 293 degrees
- Boundary layer height 800m, ground heat flux 0W/m^2, i.e. neutral conditions
- Surface roughness 0.1m

Output is normalised power deficit at each receptor (i.e. turbine location) for each flow case, with reference to the power output available from the upstream flow.

4.3.3 Results

The results shown for each flow case are graphs of the observed and modelled normalised power output for each turbine column, averaged over the inner 7 turbines in each column and graphs of the observed and modelled normalised power output for each turbine for wind directions 263, 278 and 293 degrees. In addition, Figure 27 and Figure 28 show contour plots of modelled wind speed deficit and meandering-induced turbulent velocity σ_U for U=6m/s and wind directions 263 and 278 respectively.

The model results show generally good agreement with measurements, though there is a tendency in the model to under-predict the sharp fall in power production between the first and second turbines in a row, and to over-predict the subsequent turbine-to-turbine power reduction along the row. This is most true when the wind direction is aligned with the turbine rows.

In many cases, the measurements show a lateral gradient in power production along the upstream column, which is not due to wake effects and is therefore not simulated by the model. This gradient could be caused by the non-uniform fetch along the upstream edge of the wind farm for some wind directions due to the location of the wind farm near to the coast of Denmark (see Figure 18).

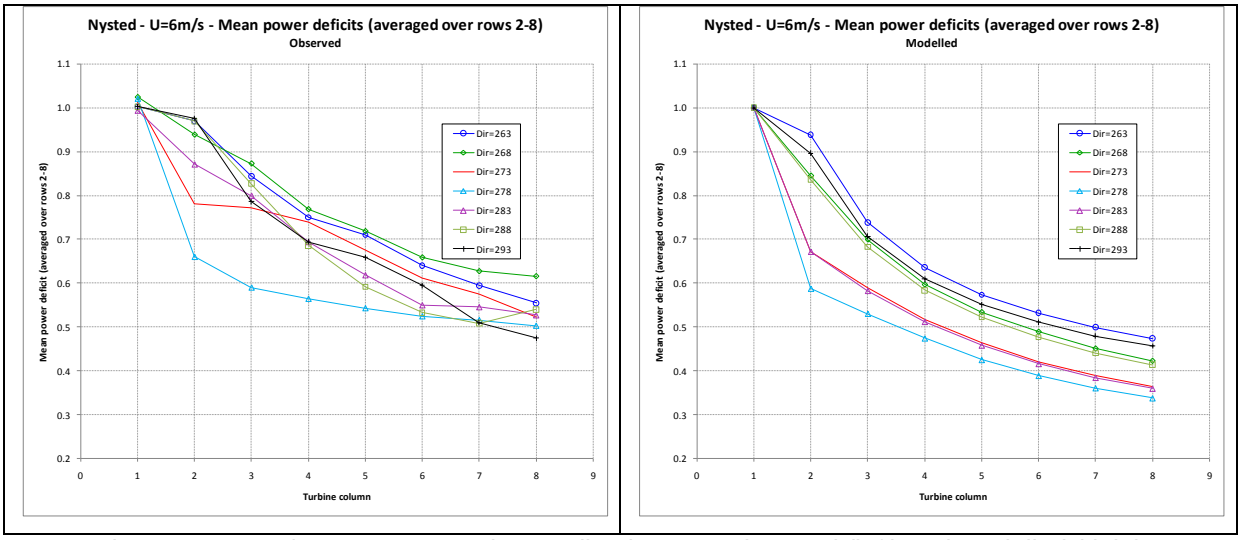

Figure 21 U=6m/s: Row-averaged normalised power; observed (left) and modelled (right)

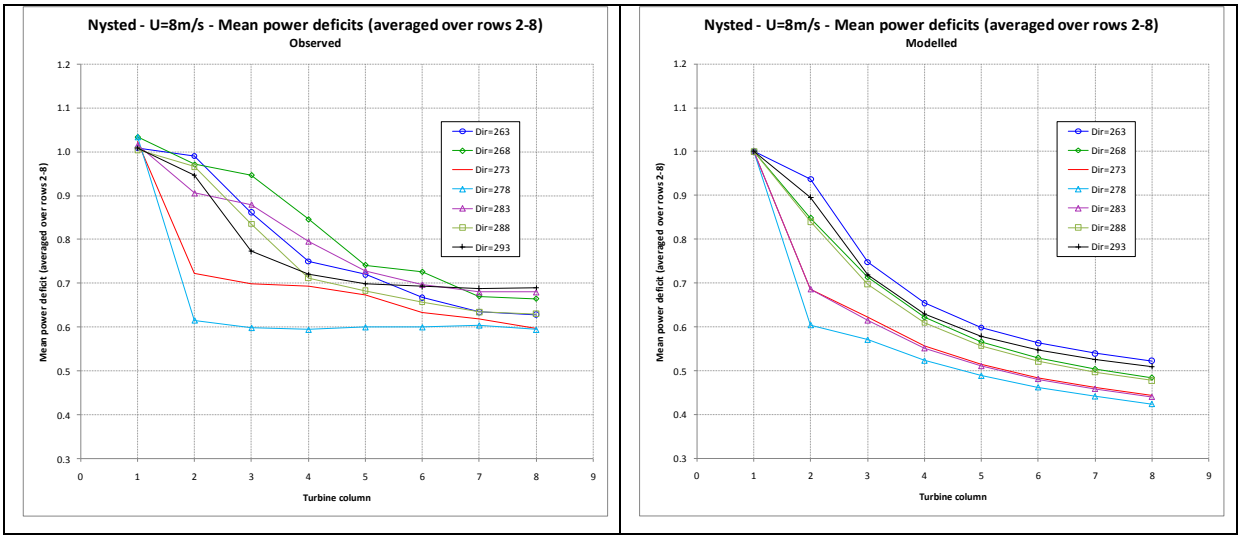

Figure 22 U=8m/s: Row-averaged normalised power; observed (left) and modelled (right)

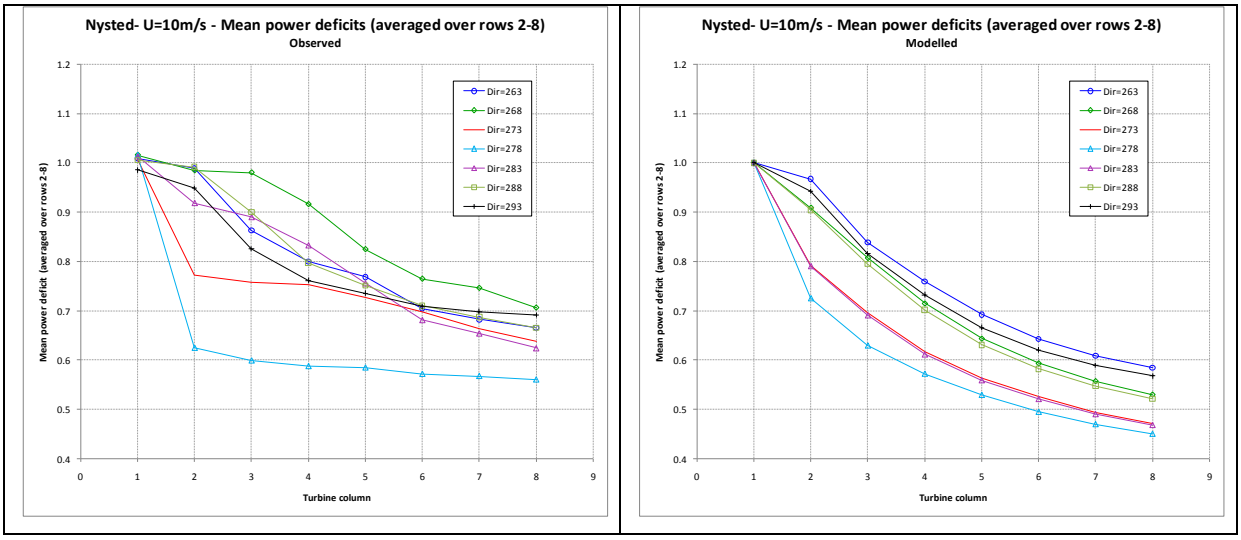

Figure 23 U=10m/s: Row-averaged normalised power; observed (left) and modelled (right)

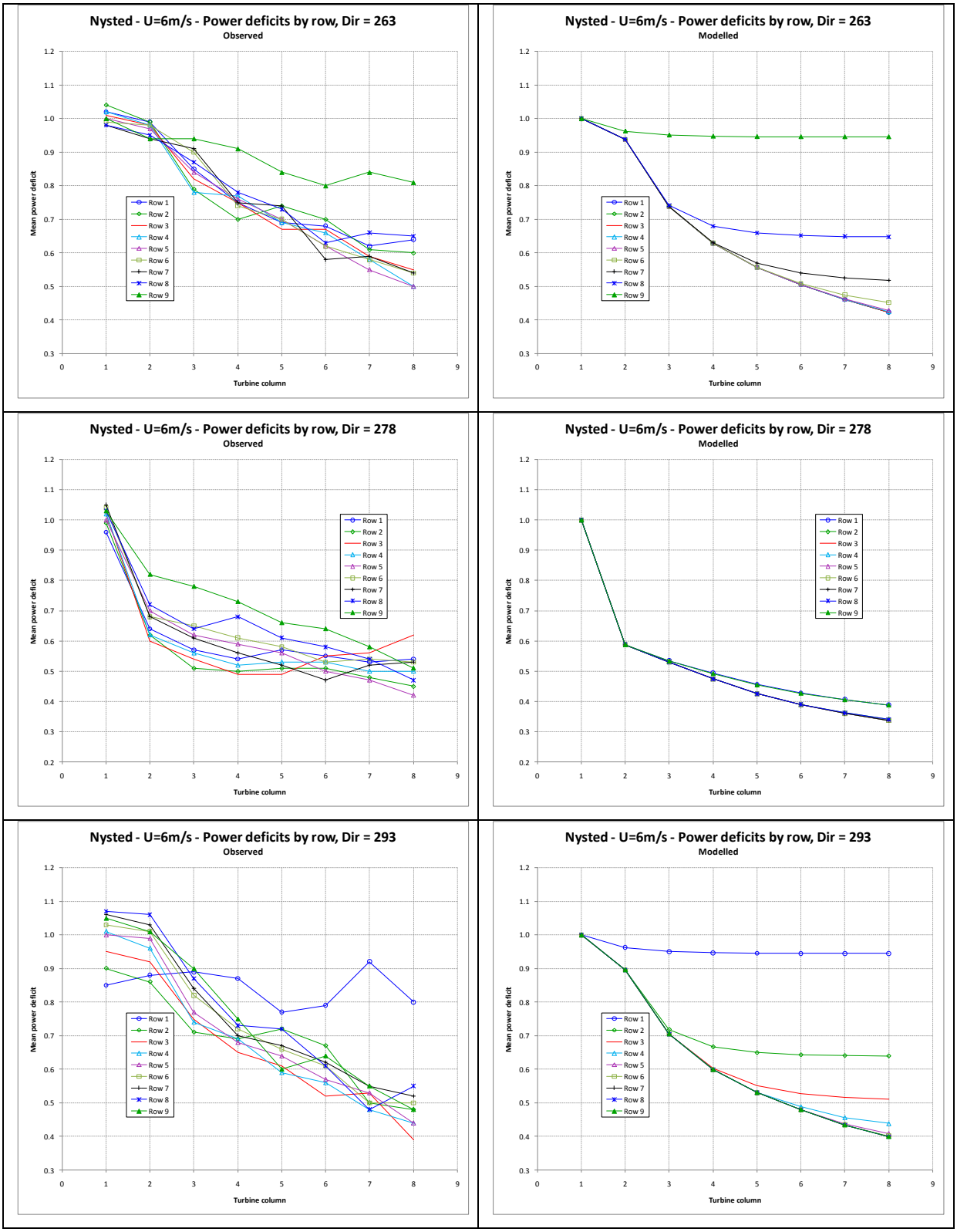

Figure 24 U=6m/s: Normalised power by row for wind directions 263, 278 and 293 degrees; observed (left) and modelled (right)

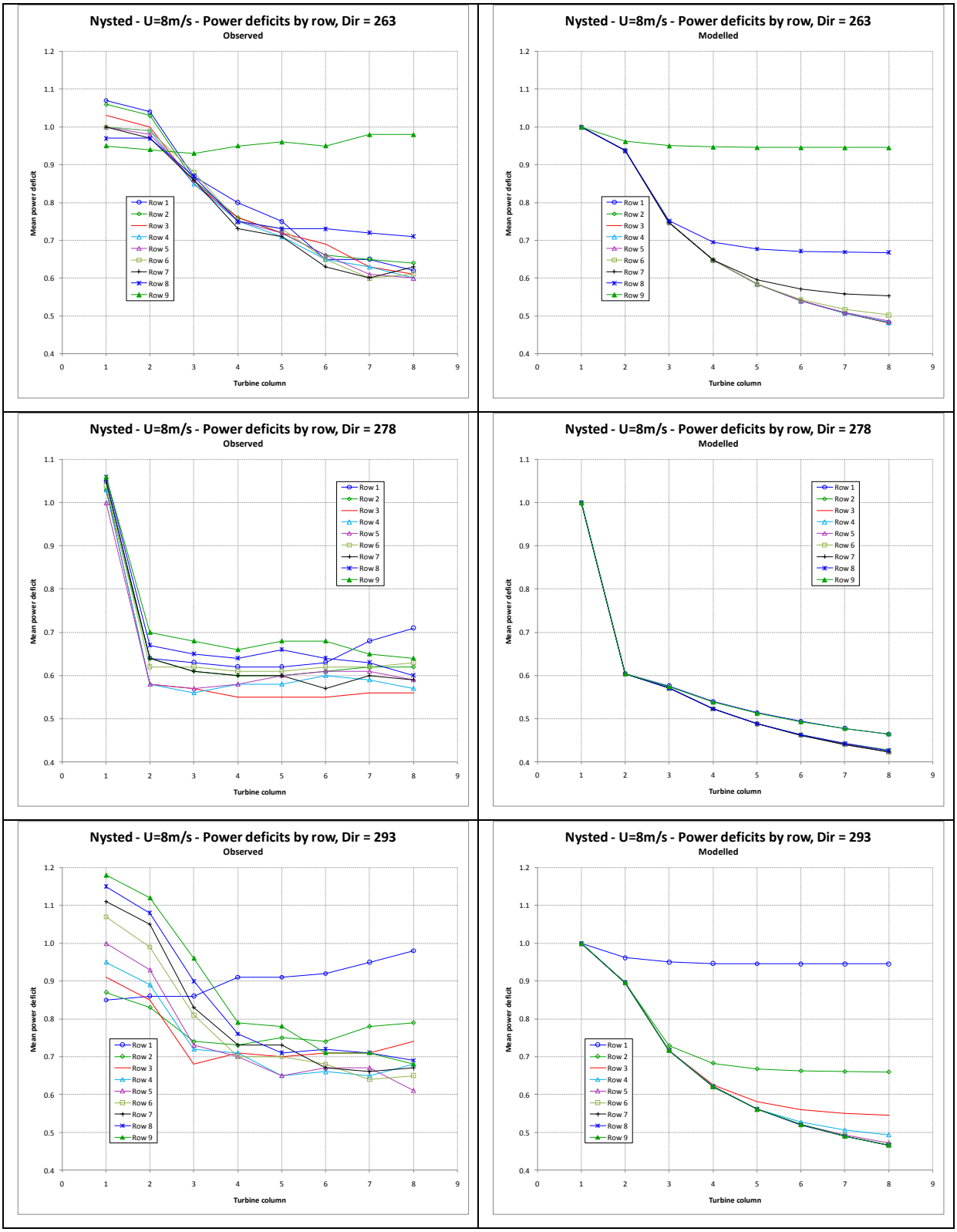

Figure 25 U=8m/s: Normalised power by row for wind directions 263, 278 and 293 degrees; observed (left) and modelled (right)

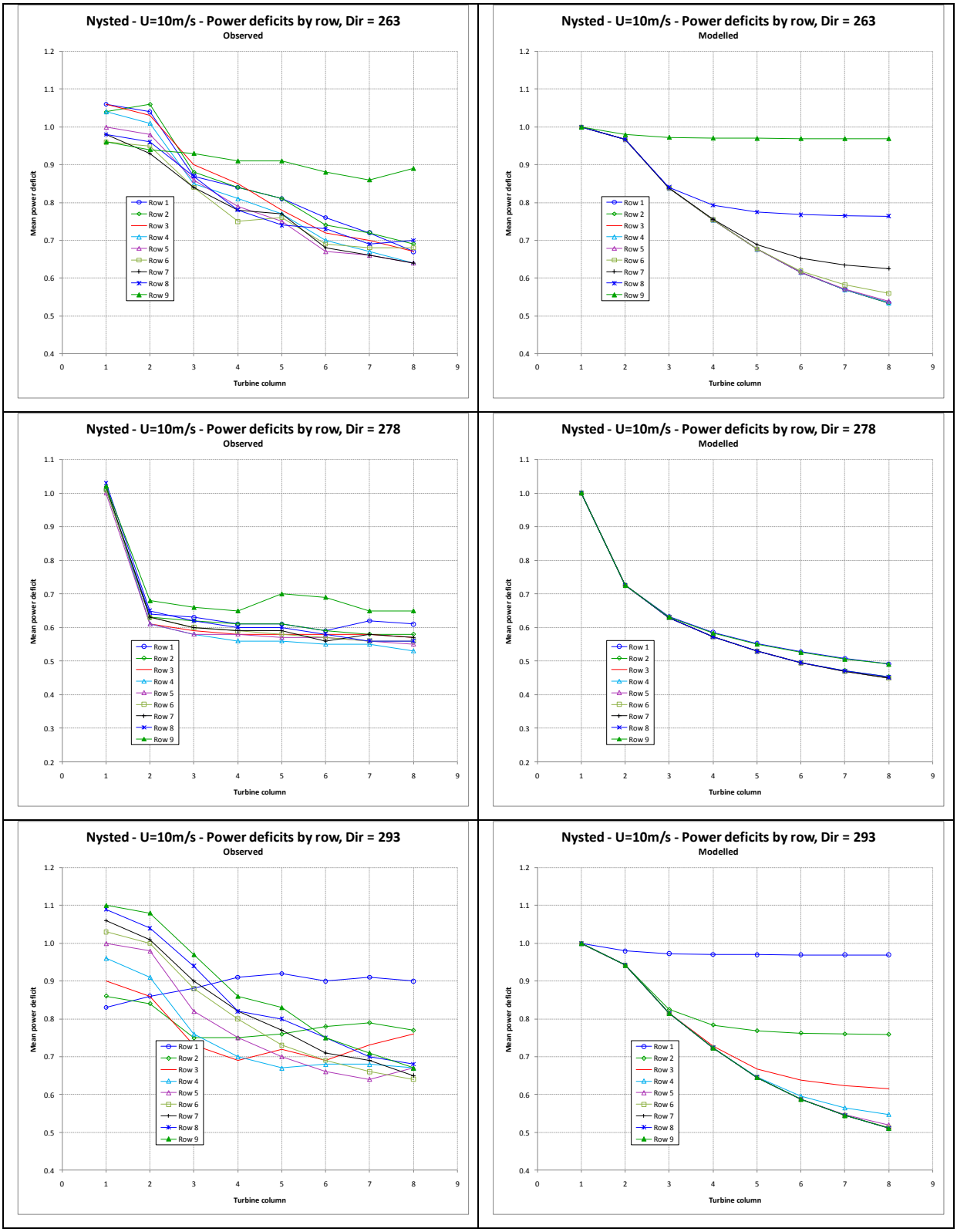

Figure 26 U=10m/s: Normalised power by row for wind directions 263, 278 and 293 degrees; observed (left) and modelled (right)

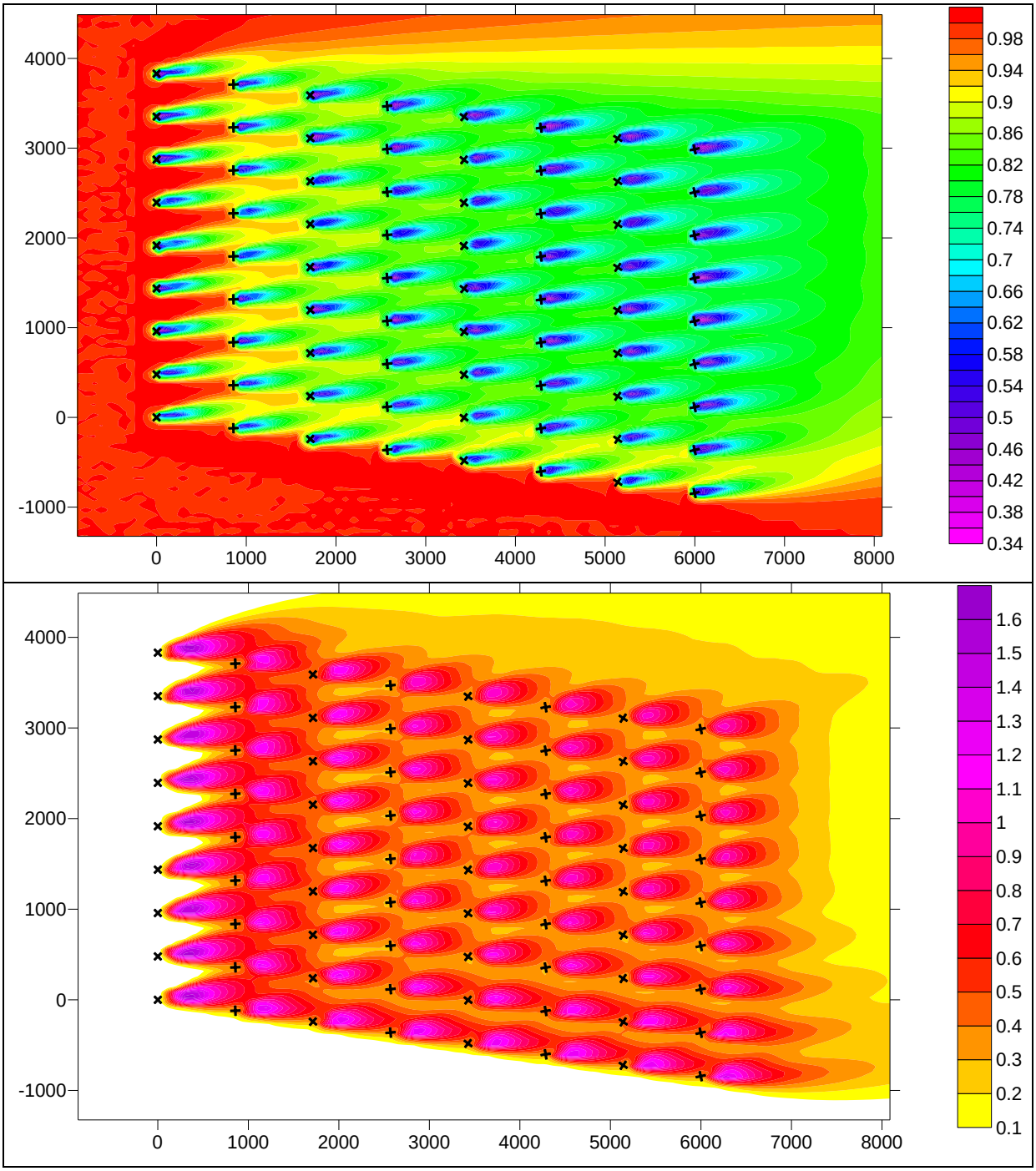

Figure 27 U=6m/s, wind direction 263 degrees: Modelled normalised wind speed (top) and meandering-induced σ_U (m/s, bottom). Crosses mark the locations of the turbines.

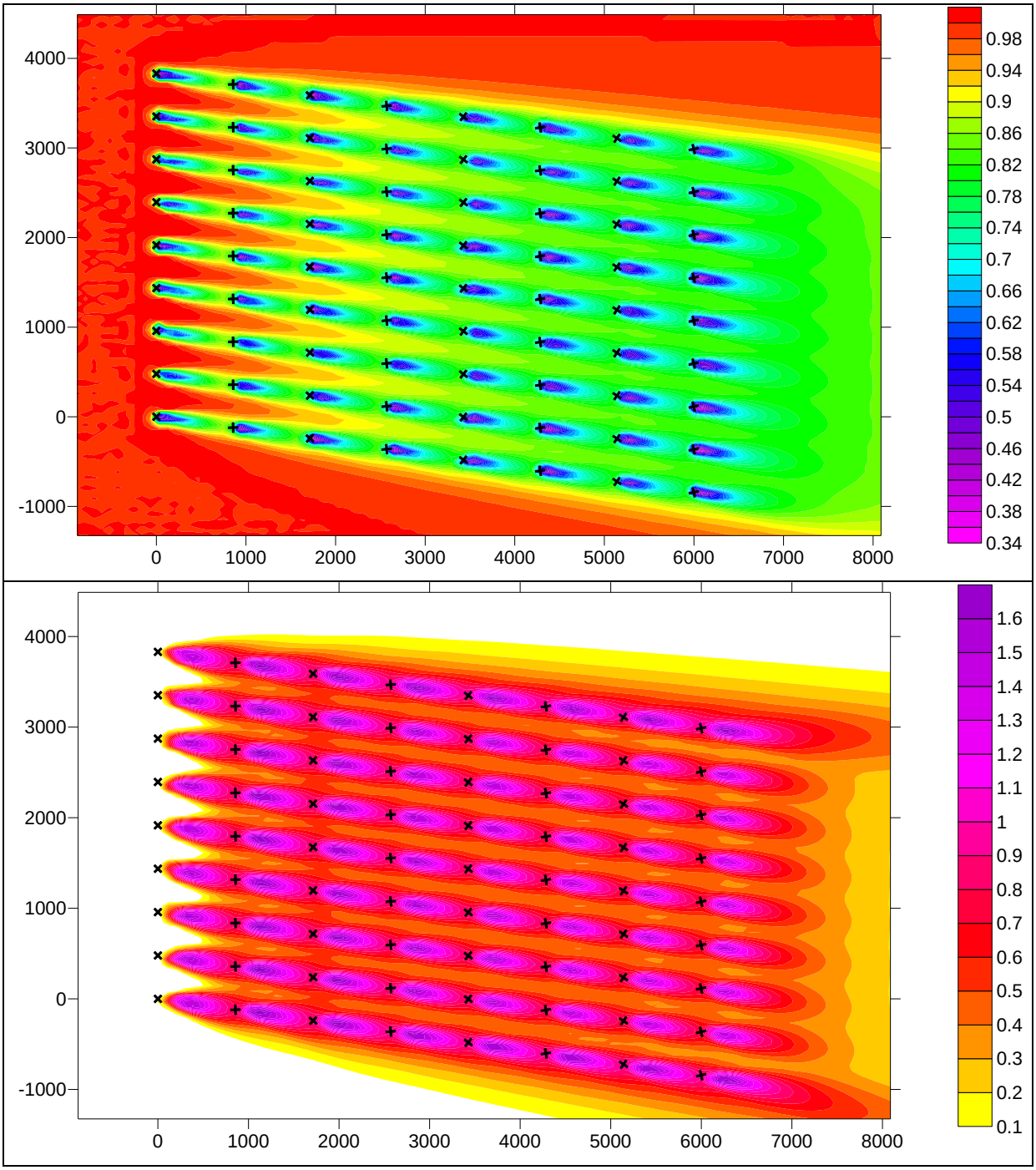

Figure 28 U=6m/s, wind direction 278 degrees: Modelled normalised wind speed (top) and meandering-induced σ_U (m/s, bottom). Crosses mark the locations of the turbines.

4.4 NoordZee wind farm

4.4.1 Site information

The NoordZee wind farm is an offshore wind farm consisting of 36 V90 VESTAS 90m, 3MW wind turbines. Each turbine has diameter 90m and hub height 70m. The turbine layout is an irregular grid, with 4 SE-NW columns containing an unequal number of turbines. The spacing between turbines in each column is 7D (where D is the turbine diameter), apart from an 11D spacing between turbines 4 and 5 in columns 2, 3 and 4. The wind farm layout is shown in Figure 29. The turbine power and thrust curves are given in Figure 30.

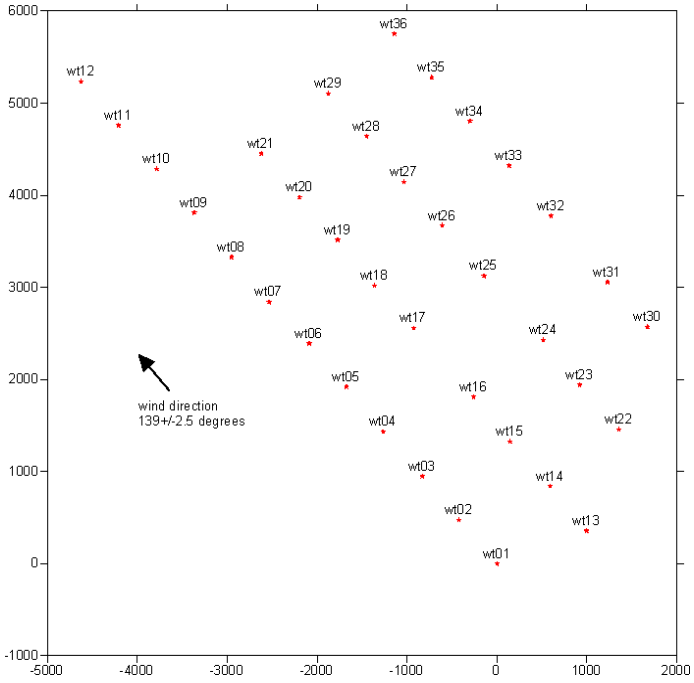

Figure 29 Layout of wind turbines in the NoordZee wind farm. Distance unit is metres; (0,0) is the location of turbine wt01. Arrow shows the wind direction case for which turbine measurements are available.

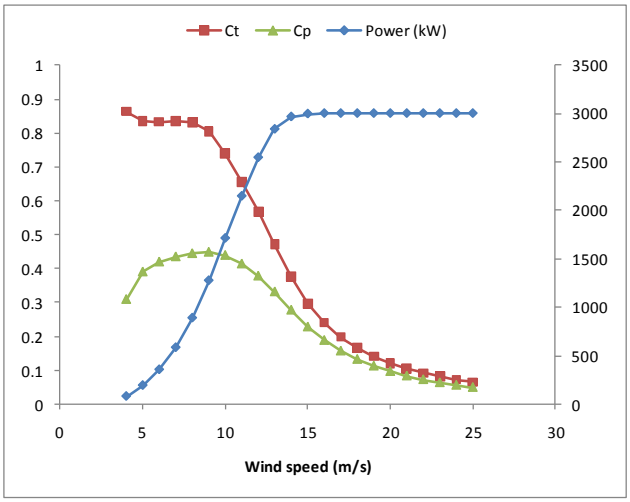

Figure 30 Power output (kW), power coefficient C_p and thrust coefficient C_T as a function of inflow wind speed for the V90 VESTAS 3MW turbines installed at the NoordZee wind farm.

The measurement data available for the wind farm are mean power output at each turbine for one wind direction case, 139±2.5 degrees, for three hub height wind speed cases: 6, 8 and 10m/s.

4.4.2 Model setup

The inputs to ADMS were as follows:

- 36 turbine sources, locations as shown in Figure 29
- Turbine height 70m
- Turbine diameter 90m
- C_p as a function of wind speed (see Figure 30)
- C_T as a function of wind speed (see Figure 30)
- Output receptors at each turbine location at hub height
- 3 flow cases: U=6, 8 and 10m/s
- Wind direction 139 degrees
- Boundary layer height 800m, ground heat flux 0W/m^2, i.e. neutral conditions
- Surface roughness 1m

Output is power deficit at each receptor (i.e. turbine location) for each flow case, with reference to the power output available from the upstream flow.

4.4.3 Results

Below are graphs of observed and modelled normalised power at each turbine for each of the three flow cases. The observed value for each turbine in a particular column is the power produced by that turbine divided by the power produced by the upstream turbine in that column (turbine 1 for columns 1 and 2, turbine 2 for column 3 and turbine 3 for column 4). The same is true for the modelled values, but because the model assumes spatially-uniform upstream flow the power produced by the upstream turbines is the same.

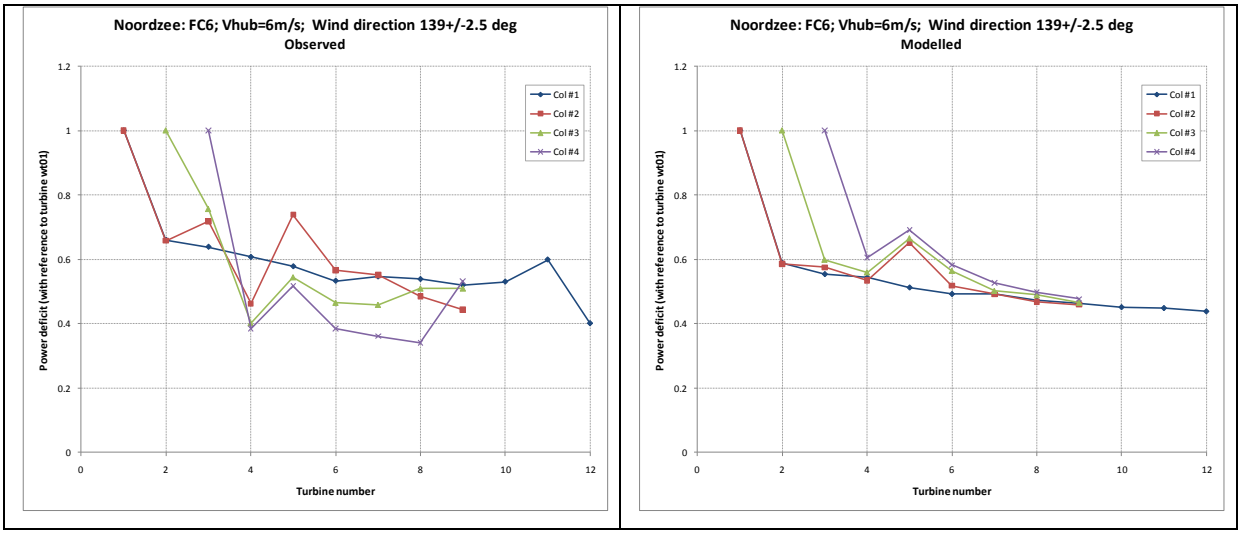

Figure 31 U=6m/s: Observed (left) and modelled (right) normalised power at each turbine.

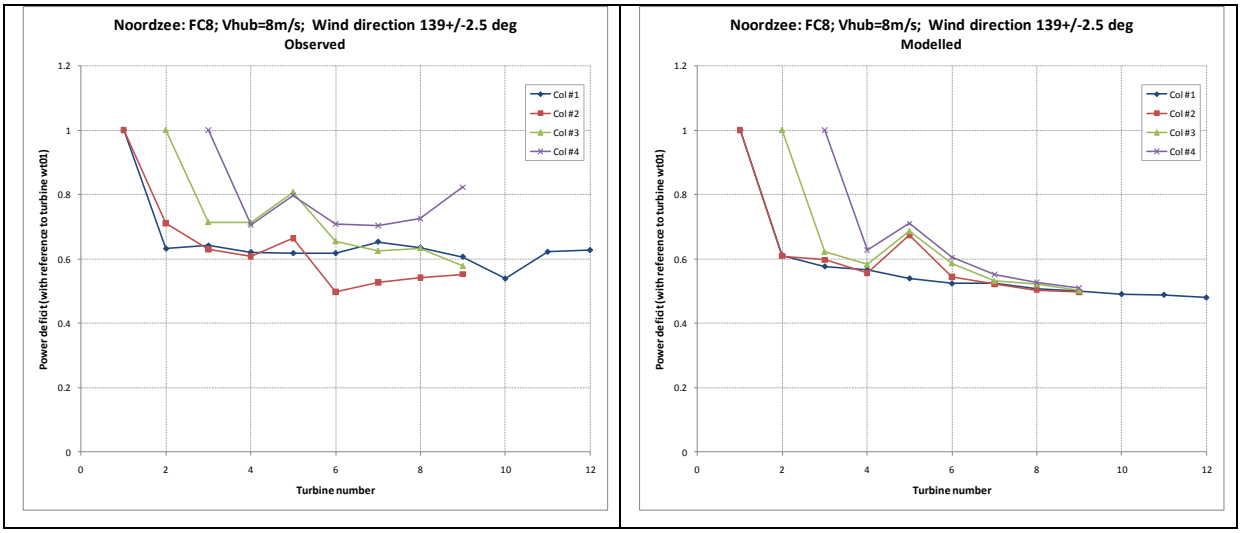

Figure 32 U=8m/s: Observed (left) and modelled (right) normalised power at each turbine.

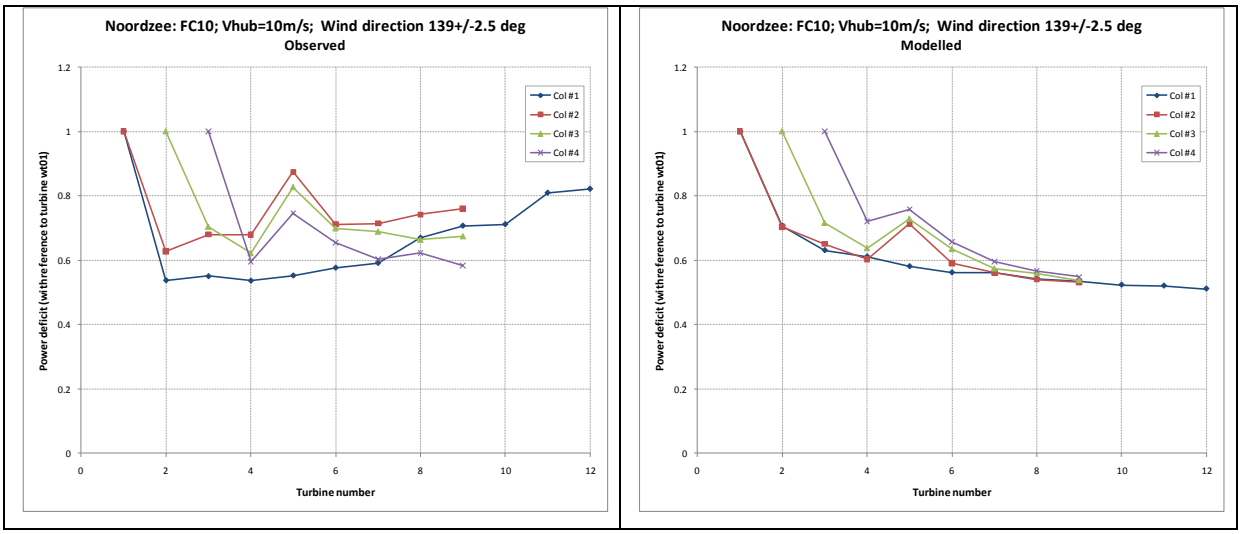

Figure 33 U=10m/s: Observed (left) and modelled (right) normalised power at each turbine.

The model generally agrees well with observations; in particular it captures well the increase in production between turbines 4 and 5 in columns 2, 3 and 4 due to the larger spacing between turbines 4 and 5 in these columns.

For the 6 and 8m/s flow cases the model captures well the sharp decline in power production between the first and second turbines in each column, and then the more gradual reduction in power production through the wind farm due to the effect of the wakes. However, for the 10m/s flow case the observations show the same sharp reduction in power production between the first and second turbines in each column, but then an unexplained gradual increase through the wind farm, which is not simulated by the model.

Contour plots of gridded normalised wind speed and meandering-induced turbulence for the U=6m/s flow case are presented in Figure 34 and Figure 35 respectively. The ambient level of along-wind turbulence in this case is only 1.3m/s, so with values of up to 1.9m/s these results demonstrate the significance of meandering-induced turbulence.

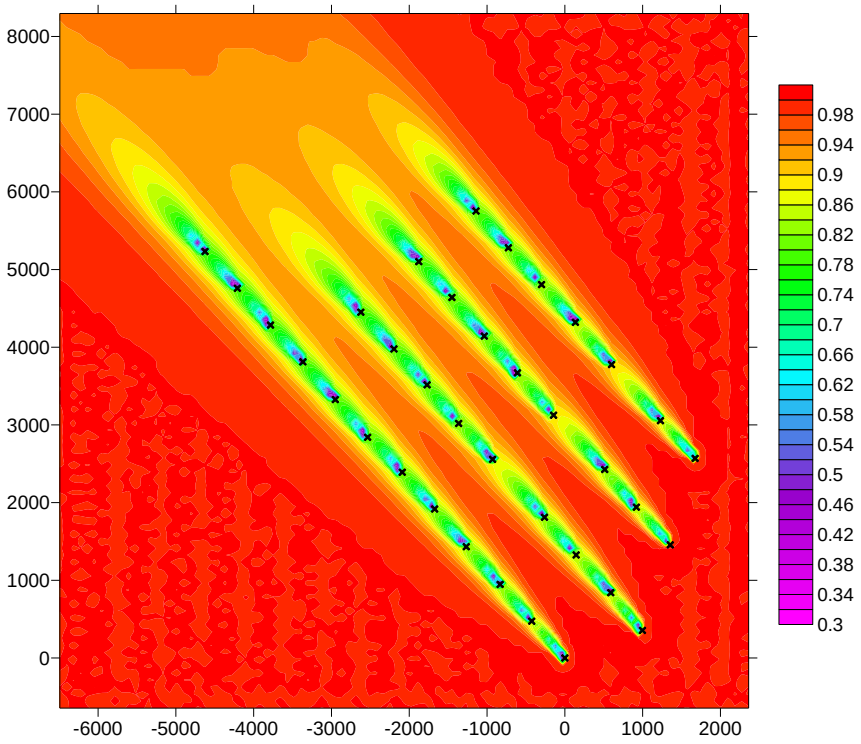

Figure 34 U=6m/s: Contour plot of modelled normalised wind speed across the wind farm ($U_{local}/U_{upstream}$). Crosses mark the locations of the turbines.

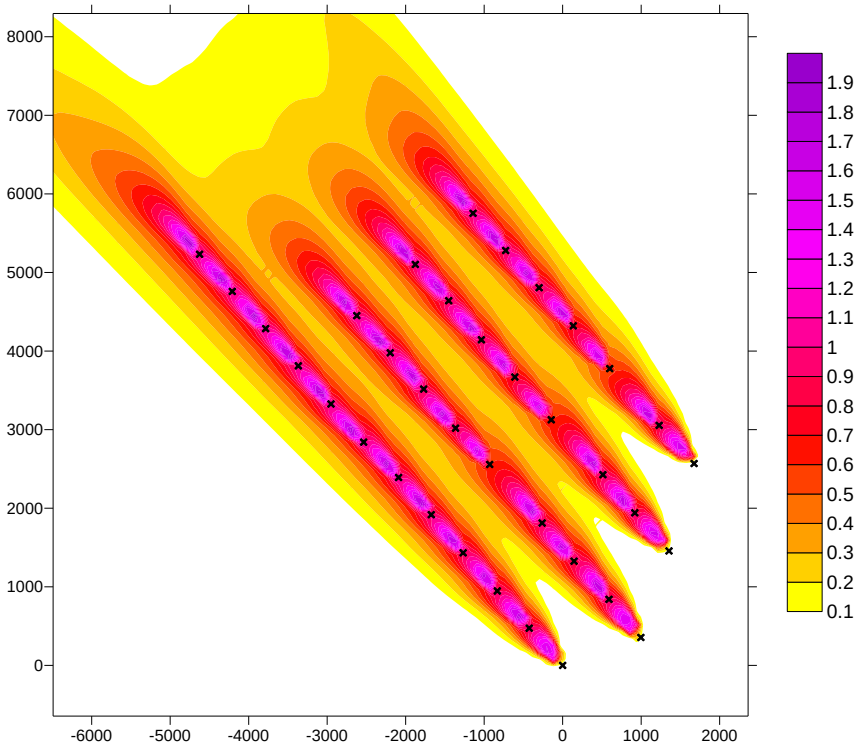

Figure 35 U=6m/s: Contour plot of modelled meandering induced turbulence (m/s) across the wind farm. Crosses mark the locations of the turbines.

5. Conclusions

During the TOPFARM project ADMS has been successfully applied to the problem of modelling wind turbine wakes, both in terms of the wind speed deficit in the wake and the additional turbulence generated by the meandering wake. The model is easy to use and quick to run for both individual wind turbines and whole wind farms. Validation work carried out shows that the model predicts wake-affected wind fields and power output figures that agree well with observations.

Areas where the model could be improved centre around the levels of turbulence in the wake. In general, the validation has shown that in the interior of a wind farm the model under-predicts the sharp reduction in power output between the first and second turbine in a row of turbines aligned with the wind and over-predicts the reduction in power between subsequent turbines.

In addition to work to improve the performance of the model against validation datasets, future work on the ADMS turbine wake model may include:

- The ADMS wake model will be implemented in the ADMS complex terrain model, FLOWSTAR, to properly account for variations in terrain and surface roughness.

- Currently when a wind farm is modelled in ADMS the vertical profiles of wind speed and σ_U for each turbine are modified to include the effect of upstream wakes. A different vertical profile is used for each turbine, but the dispersion of each wake uses a horizontally uniform flow field. The model will be developed so that the dispersion of each wake uses a 3-dimensional flow field that includes the horizontal variation in the wake-affected flow field as well as vertical variations.

- The standard ADMS pollution dispersion algorithms will be developed to use the modelled wake-affected wind and turbulence fields to disperse pollutants released into the atmosphere. In addition, the capability of ADMS to calculate turbine power output will be developed to enable calculation of the effect of the modified flow field around site buildings on the power production of nearby wind turbines.

6. References

6.1 ADMS references

Information about ADMS: http://www.cerc.co.uk/environmental-software/ADMS-model.html

ADMS documentation, including User Guide and Technical Specification documents: http://www.cerc.co.uk/environmental-software/model-documentation.html

Chapters of the ADMS Technical Specification of particular relevance:

1. P13/07, 'Concentration fluctuations in ADMS 3 and ADMS 4, including fluctuations from anisotropic and multiple Sources': http://www.cerc.co.uk/environmental-software/assets/data/doc_techspec/CERC_ADMS4_P13_07.pdf
2. P05/01, 'The Meteorological input module': http://www.cerc.co.uk/environmental-software/assets/data/doc_techspec/CERC_ADMS4_P05_01.pdf
3. P25/03, 'Implementation of area, volume and line sources': http://www.cerc.co.uk/environmental-software/assets/data/doc_techspec/CERC_ADMS4_P25_03.pdf

Carruthers DJ, Hunt JCR and Weng W-S, **1988**: 'A computational model of stratified turbulent airflow over hills – FLOWSTAR I'. Proceedings of Envirosoft. In Computer Techniques in Environmental Studies (editor P. Zanetti), pp. 481-492. Springer-Verlag.

6.2 Wind turbine wake references

Martin O. L. Hansen, 'Aerodynamics of wind turbines', Second Edition (2008), published by earthscan.

Tony Burton, David Sharpe, Nick Jenkins and Ervin Bossanyi, 'Wind Energy Handbook', First Edition (2008), published by John Wiley & Sons.

Paul M. Bevilaqua and Paul S. Lykoudis "Turbulence memory in self-preserving wakes", Journal of Fluid Mechanics, Volume 89, Issue 03, December 1978, pp 589-606

6.3 Acknowledgements

We would like to offer sincere thanks to all the partners in the TOPFARM project, who were all generous enough to share their knowledge and experience to help us understand the basics of wind farm engineering.

Particular thanks go to Kurt Hansen at DTU Denmark for all his help with the turbine measurement datasets.